A VISUAL SYSTEM OF TECTAL ORIGIN IN THE MAMMALIAN BRAIN

Ph.D. Thesis

Attila Nagy

Department of Physiology, General Medical Faculty, University of Szeged, Szeged

2003

1. List of publications related to the subject of the thesis

I. Benedek G, Norita M, Hoshino K, Katoh YY, Eördegh G, **Nagy A** (2003) Extrageniculate visual pathways in the feline brain. In: Dumitrascu DL (editor) Psychosomatic Medicine; Recent progress and current trends. "Iuliu Hatieganu" University Publishing House, Cluj, Romania, pp 33-40. ISBN: 973-8385-62-8

II. **Nagy A**, Eördegh G, Benedek G (2003) Spatial and temporal visual properties of single neurons in the feline anterior ectosylvian visual area. Exp Brain Res 151:108-114

III. **Nagy A**, Eördegh G, Masao N, Benedek G (2003) Visual receptive field properties of neurons in the feline caudate nucleus. Eur J Neurosci 18:449-452

IV. **Nagy A**, Eördegh G, Benedek G (2003) Extents of visual auditory and bimodal receptive fields of single neurons in the feline visual associative cortex. Acta Phys Hung (in press)

Table of contents

1. Introduction

The notion of the existence of a multimodal sensory area over the anterior part of the cat brain is not novel. It was put forward first by Loe & Benevento (1969). The story of the ectosylvian visual pathway started in 1980 when Otto Creutzfeldt & Lennart Mucke attempted to record visual neurons in the claustrum via stereotaxic targeting. They were repeatedly able to record visually highly active neurons, but on histological control these turned out to be located outside the border of the caudal portion of the claustrum. This serendipitous finding yielded to the discovery of a novel visual area along the anterior ectosylvian sulcus (AES) (Mucke et al., 1982) and initiated experiments clarifying the extrageniculate visual pathways of the feline brain. It should be noted that Olson & Graybiel (1983), who had similarly searched for visual activity in the claustrum, simultaneously detected the existence of the anterior ectosylvian visual area (AEV) (1983). Later, the visual region was extended to the cortex throughout almost the whole length of the AES, including its rostral gyral cortical region; this was called the insular visual area (IVA) (Benedek et al., 1986; Hicks et al., 1988a; b; Norita et al., 1991), a name that was later found to be not totally appropriate (Reinoso-Suares & Roda, 1985).

The existence of separate geniculate and extrageniculate visual systems in the feline brain has been proved in both morphological and physiological studies. Besides the lateral geniculate nucleus, a total of nine subcortical structures have been found that receive afferents directly from the retina (Rosenquist, 1985). Of these structures, the superior colliculus (SC), whose neurons provide the origin for the tectal extrastriatal pathway, has attracted most research interest in the course of the past twenty years. During this period, the morphological and physiological properties of the extrageniculate pathway in the cat brain have been described in detail.

1.1. Morphological connections within the extrageniculate pathways

Morphological experiments have confirmed the tectal source of visual information toward the AEV (Harting et al., 1992). This area now seems to be the only cortical visual area provided with visual that afferentation entirely bypasses the lateral geniculate complex (Rosenquist, 1985). The excitatory Y inputs from the retinal ganglion cells dominate the responses of neurons in the SC and AEV (Wang et al., 1998; 2001). The AEV receives thalamic afferents mainly from the lateralis medialis-suprageniculate nuclear complex (LM-

Sg), a smaller proportion of the afferentation coming from the medial part of the nucleus lateralis posterior (LPm) (Norita et al., 1986). The main source of the cortical afferentation to the AEV is the posterior-medial division of the lateral suprasylvian (PMLS) area (Miceli et al., 1985; Norita et al., 1986). The predominant targets of efferentation of the visual neurons along the AES are the LM-Sg and the intermediate and deep layers of the SC, although it provides visual efferents to the PMLS area, to the frontal eye fields, to the amygdala and other cortical and subcortical structures, out of the lateral geniculate complex and the A17 region (Norita et al., 1986; Harting et al., 1992). The heavy corticothalamic connections directed attention to the LM-Sg. This nucleus of the posterior thalamus has evaded thorough morphological and physiological analysis because of problems with the definition of its borders. Acetylcholinesterase staining provided a possibility to circumscribe and locate this thalamic area exactly (Hardy et al., 1976). Anatomical tracing experiments proved that there is a noteworthy convergence of inputs from a wide anteroposterior and mediolateral aspect of the intermediate and deep layers of the SC to the neurons in the LM-Sg (Katoh & Benedek, 1995). Fluorescein double-staining experiments indicated that collicular neurons send bifurcating axons towards the LM-Sg in both hemispheres (Katoh et al., 1995). Morphological experiments revealed that both the fastigial nuclei of the cerebellum (Katoh et al., 2000; Katoh & Benedek, 2003) and the pedunculopontine tegmental nucleus (PPT) send efferents (Hoshino et al., 2000) to the ventral part of the LM-Sg. Further heavy projection has been traced from the ventral LM-Sg to the dorsolateral part of the caudate nucleus (Harting et al., 2001a; b). This finding extended our observations to the caudate nucleus, a part of the brain that can directly be involved in visuomotor control (Brown et al., 1995; Niida et al., 1997; Harting et al., 2001a; b; McHaffie et al., 2001). Further, the substantia nigra dopaminergic and non-dopaminergic neurons receive tectal afferentation from the intermediate and deep layers of the SC through direct (Comoli et al., 2001) and indirect (Redgrave et al., 1987; Tokuno et al., 1994; Lokwan et al., 1999) pathways. Figure 1 shows the most relevant morphological connection within the extrageniculate visual system.

1.2. Physiological properties of the extrageniculate cortical and subcortical regions

Physiological experiments were started immediately after the detection of visually active neurons in the AEV. All the experiments were performed on anesthetized, immobilized, artificially respirated cats with extracellular single unit recordings. Early observations demonstrated that the AEV neurons possess particular receptive field properties

(Mucke et al., 1982; Benedek et al., 1988). The visual neurons are mostly located on the ventral bank of the AES (Jiang et al., 1994). Very similar receptive field properties have been found in neurons in the IVA (Benedek et al., 1986; Hicks et al., 1988b), in the retino-recipient intermediate and deep layers of the SC (Stein & Meredith, 1993) and in the LM-Sg (Benedek et al., 1997). Hence, we can summarize the visual receptive field properties, irrespectively of the region in question. A striking physiological characteristic of these neurons (i.e. in the AEV, IVA, LM-Sg and SC) is the overwhelming sensitivity of the neurons to movement in their receptive field. The neurons are primarily sensitive to very small stimuli moving very rapidly in a specific direction in their huge receptive field (Benedek et al., 1988; 1997; Hicks et al., 1988b). A substantial proportion (approximately 20%) of the AEV neurons respond optimally to stimuli moving at a speed of higher than 1000 degree/second (deg/s). No other area of the cat cortex contains such a high proportion of neurons that respond optimally to very fast stimuli. Most of the neurons are highly direction-selective. The AEV appears to contain the neurons with the highest directional selectivity indices in the feline brain (Benedek et al., 1986; 1988; 1997). Several neurons have also been found that failed to show end-inhibition properties and ones that did not prefer extremely high stimulus velocities, but clearly no neuron was observed which exhibited the velocity properties demonstrated in the striate area (Benedek & Hicks, 1988). Thus, two major types of neurons can be distinguished along the extrageniculate pathway, and particularly in the AES region. There are neurons with a preference for high velocities and additionally with "transient" or "phasic" response properties. These neurons are abundant in the "deep" sulcal part of the AES. The neurons of the other type possess a less excessive velocity sensitivity and their response is characteristically of "tonic" type (Benedek & Hicks, 1988). These neurons have consistently been detected in the IVA region. Most of the neurons were not responsive or elicited much weaker responsivity to stationary stimulation (Mucke et al., 1982; Benedek et al., 1986; 1997). Accordingly it is not easy to draw the exact borders of the receptive fields. Although the visual receptive field properties have been extensively investigated, the visual receptive field size and retinotopical organization within the AEV remain a matter of controversy. Some studies have indicated the complete absence of retinotopic organization (Mucke et al., 1982; Benedek et al., 1988; Hicks et al., 1988b) in contrast with the impressive retinotopy in the geniculostriatal pathway (Tusa et al., 1978). Olson & Graybiel (1987) described a limited retinotopic organization in the AEV, as indicated by the fact that the receptive fields gradually shift with tangential movement of the microelectrode through the cortex. Others have raised the possibility that the neurons in the AEV are arranged according to their directional

preference (Scannel et al., 1996). Different attempts to draw the borders of the visual receptive fields of the AES neurons have yielded widely differing results. Olson & Graybiel (1987) reported that the mean visual receptive field diameter of the AEV neurons is 15° and that the receptive fields are mostly located in the lower contralateral quadrant. Scannel et al. (1996) similarly found relatively small receptive fields (mean=18°), but their results revealed that the receptive fields extended up to 10° into the ipsilateral hemifield. Benedek et al. (1988) demonstrated that the visual neurons in the AES have extremely large receptive fields, which consistently include the area centralis and cover almost the whole visual field of the eye involved. All of these receptive field mappings resulted from subjective observations, where the stimuli were generated with hand-held lamps and projectors. Hence an objective description of the extents of the visual receptive fields of the AEV neurons is still missing.

An interesting aspect of the tecto-thalamo-cortical system is its sensitivity to various sensory modalities. The multimodal character of the intermediate and deep layers of the SC has been extensively studied (Meredith & Stein, 1986; Meredith et al., 1992). It emerged that there is a heavy representation of auditory and somatosensory modalities in both the LM-Sg and the cortex along the banks of the AES (Hicks et al., 1988a; Jiang et al., 1994; Benedek et al., 1997). Neurons along the AES that display auditory sensitivity are mainly concentrated on the banks and fundus of the posterior three-quarters of the AES (Jiang et al., 1994). The extents of the auditory receptive fields in the AEV were investigated by Middlebrooks et al. (1994; 1998; 2002), whose observations demonstrated that the auditory receptive fields are extremely large, covering 360° of azimuth of the horizontal plane. No preferred type or frequency of auditory stimulation was observed. The somatosensory receptive fields are also large. Somatosensory neurons can be activated by stimulation of the whole contralateral body surface and some have receptive fields extending even to the ipsilateral body surface. No receptive field organization has been detected (Benedek et al., 1996). Somatosensory neurons are mostly located in the anterior two-thirds of the dorsal bank of the AES (Jiang et al., 1994). A high number of bimodal and even trimodal cells have been found too (Benedek et al., 1996; 1997). Detailed analyses of the bimodal neuronal responses revealed the existence of cross-modal interactions between auditory and visual modalities. In most cases, multisensory cross-modal facilitation was described, although multisensory inhibition has been observed as well (Hicks et al., 1988a; Wallace et al., 1992; Stein & Wallace, 1996).

1.3. Spatial coding abilities of the AES neurons

The stimulus-source location ability is an important aspect of neurons along the extrageniculate pathways. The topographical code and retinotopical organization assumed that single neurons are selective for particular stimulus locations and the stimulus-source locations are coded by the cortical location of a small population of maximally activated neurons (Tusa et al., 1978; Middlebrooks et al., 1998). The absence of traditional topographic coding and retinotopical organization in the AES cortex gave rise to the idea that there could be another type of spatial coding in this system. Middlebrooks et al. (1994; 1998; 2002) described distributed population coding for sound-source location in the auditory neurons along the AES. The distributed code assumes that the individual neurons are panoramic localizers and can carry information about stimulus locations throughout 360^{o} of azimuth. These neurons reportedly have the potential to code the location of a sound stimulus within their huge receptive field. The accurate sound-source localization stems from information that is distributed across a large population of such panoramic neurons (Midlebrooks et al., 1998). For visual stimulus-source location in a restricted part of the visual field, evidence was also found for the distributed code (Benedek et al., 2000).

1.4. Behavioral and functional role of the extrageniculate visual system

Despite the large number of studies that have described the physiological and morphological properties of the AEV neurons, the behavioral role of the AEV and the extrageniculate visual system has not yet been clarified. Tamai et al. (1989) observed that intracortical microstimulation of the AEV evoked centering movements of both eyes. Thus, they suggested that the AEV might be involved in the control of eye movements. As mentioned earlier, the AEV projects strongly into the deep layers of the ipsilateral SC (Harting et al., 1992). The superior colliculi in turn, and especially the deep layers, play an important role in visual guided eye movements (for a review, see Stein & Meredith, 1991). Others have suggested that the AEV may perform a specific role in the recording of movements of the visual environment relative to the body and in the adjustment of the motor behavior to such movements (Mucke et al., 1982; Wang et al., 1998). Another possible functional role of the AEV can be to take part in the orientation behavior (Wilkinson et al., 1996). From these results, it can be seen that the exact behavioral role of the AEV and the

extrageniculate visual system awaits further classification. A description of the spatial and temporal properties of the AEV neurons could contribute to an understanding of how these neurons take part in visual information processing in connection with behavioral action. Although theoretical considerations require that the spatial and temporal frequency sensitivity functions fully describe the responsiveness of neurons to any kind of stimuli, no study has yet been performed that involved a systematic examination of the responses of the AEV neurons to sinusoidally modulated gratings. Only one relevant study has been reported where square-wave modulated grating stimulation was used to investigate the spatial and temporal frequency sensitivities of the neurons along the rostral part of the AES, called the insular cortex. The results, which are limited, demonstrated and showed that these neurons prefer low spatial and high temporal frequencies, but no information is available on the spatial and temporal tuning characteristics of the AES neurons (Hicks et al., 1988b).

2. Aims of the study

The aims of our experiments were to describe the receptive field properties of the AES neurons in order to achieve a better understanding of the spatial coding abilities and the functional role of the extrageniculate tecto-thalamo-cortical visual system and to extend the tecto-thalamo-cortical visual system that starts from the SC to the caudate nucleus. Our concrete aims were:

1. To give an objective description of the extents of the receptive fields of the visual, auditory and bimodal neurons along the AES.
2. To obtain evidence for the spatial coding abilities of the AEV neurons so as to acquire a better understanding of the multimodal representation of the environment in the mammalian brain
3. To record visual neurons in the caudate nucleus
4. To describe the visual receptive field properties of the caudate single neurons and to compare them with those of other visual cortical and subcortical structures in order to reveal the role of the caudate nucleus in the visual information processing.
5. To describe the spatial and temporal visual properties of the AEV neurons and to compare them with those of other visual structures, thereby clarifying the possible functional role of the AEV in connection with behavioral actions.

3. Materials and methods

3.1. Animal preparation and surgery

Experiments were carried out on 22 adult cats of either sex weighing between 2.5 and 3.5 kg. The experimental protocol had been accepted by the Ethical Committee for Animal Research of the Albert Szent-Györgyi Medical and Pharmaceutical Center of the University of Szeged. The cats were initially anesthetized with ketamine hydrochloride (30 mg/kg i.m.). The trachea was intubated, the femoral vein was cannulated and the animals were placed in a stereotaxic headholder. Wound edges and pressure points were treated generously with procaine hydrochloride (1%). The anesthesia was continued with halothane (1.6% during surgery and 0.6% during recordings). The depth of anesthesia was monitored by repeatedly monitoring the pupil size, electrocorticogram and electrocardiogram. The animals were immobilized with gallamine triethiodide (Flaxedil, 20 mg/kg i.v.). A liquid containing gallamine (8 mg/kg/h), glucose (10 mg/kg/h) and dextran (50 mg/kg/h) in Ringer's solution was infused at a rate of 3 ml/h. The end-tidal CO_2 level and the rectal temperature were monitored continuously and kept approximately constant, at 3.8-4.2% and 37-38 °C, respectively. The skull was opened with a dental drill to allow a vertical approach to the AEV and the caudate nucleus. The dura was covered with a 4% solution of agar dissolved in Ringer solution at 38 °C. The eye contralateral to the cortical recording was treated with phenylephrine (10%) and atropine (0.1%) and was equipped with a +2 diopter contact lens. The ipsilateral eye was covered during stimulation. A subcutaneous injection of 0.2 ml 0.1% atropine was administered preoperatively.

3.2. Recording

Electrophysiological recording of single units in the AEV and the caudate nucleus was carried out extracellularly via tungsten microelectrodes (AM System Inc. USA, 2-4 MOhm). Single-cell discrimination was performed with a spike-separator system (SPS-8701, Australia). Neuronal activities were recorded and correlated with the movement of the light stimulus by a computer and stored for further analysis as peristimulus time histograms (PSTHs). Vertical penetrations were performed between the Horsley-Clarke co-ordinates anterior 12-17 and lateral 4-6.5 in the stereotaxic depths in the interval 12-19 to record

caudate nucleus neurons and anterior 10-14 and lateral 12-14 in the stereotaxic depths in the interval 13-17 to record AEV neurons. Electrolytic lesions marked the locations of successful electrode penetrations. All of the recorded neurons were located either in the caudate nucleus or in the AES cortex.

3.3. Stimulation and data analysis to estimate the extents of the visual, auditory and bimodal receptive fields of the AEV neurons

For auditory stimulation, we used 12 loudspeakers placed at 15° intervals on the 165° perimeter before the inter-aural plane that delivered white noise (40 dB). The duration of auditory stimulation was 1 s. The visual stimulus was provided by the subsequent lighting of 12 light-emitting-diode (LED) pairs placed in the same way as the loudspeakers on the 165° perimeter, 30 cm from the eye, in an arc positioned according to the Horsley-Clarke horizontal zero plane. The light emission time of the first LED was 120 ms and this was followed immediately by emission for 320 ms by the second one. The computer-controlled stimuli were presented in a pseudo-random order, separately or simultaneously (bimodal). The interstimulus interval was 1 s. The prestimulus time (without any kind of stimulation the spontaneous neuronal activities were recorded) was 500 ms, and the peristimulus time (visual or auditory or bimodal stimuli were presented) was also 500 ms. Whenever a single unit was found that was visually or auditory-sensitive, at least 10 trials were run in each condition.

The net firing rate was calculated as the difference between the firing rate during the first 500 ms of stimulation and that before stimulation. The net firing rate was defined as a response when a t-test revealed a significant ($p<0.05$) difference between the two values. The width of the receptive field of a neuron was determined by the locations of stimuli that induced a significant response. As maximal sites we considered those stimulus localizations at which the net firing rates were the highest. We defined laterality as a significant difference in mean net firing rate between the responses to stimuli from the ipsi- and contralateral visual fields. The area centralis was at 0° on the perimeter. When the bimodal peristimulus net firing rate was found by analysis of variance (ANOVA) to be significantly higher ($p<0.05$) than the most effective single modality peristimulus net firing rate, a facilitatory interaction was considered to exist. The strength of an interaction was calculated via the formula coined by Meredith & Stein (1986):

$$\{(CM - SM_{max})/(SM_{max})\} \times 100 = \text{interaction\%}$$

where CM is the mean number of impulses evoked by the bimodal stimulus and SM_{max} is the mean number of impulses evoked by the most effective single-modality stimulus. The extents of the facilitatory bimodal interactions were determined by the locations of stimuli that induced significant multisensory facilitation.

3.4. Visual stimulation and data analysis to describe the visual receptive field properties of the caudate nucleus neurons

For visual stimulation, small spots 1° in diameter or light bars 1° in width and of four various lengths (1, 3, 5 or 10°) were generated by a projector device equipped with an adjustable slit-lamp diaphragm. The stimuli were moved with a computer-controlled moving mirror system and were projected across the tangent screen (63 cm in front of the animal) in 8 different directions (0-315° in 8 steps with 45° increments) and at 4 different speeds (15, 30, 60 and 120 deg/s). We defined the velocities according to Waleszczyk et al. (1999) as low (<20 deg/s), intermediate (20-100 deg/s) or high (>100 deg/s). Each stimulus was presented at least 15 times. Both the prestimulus time (during which stationary spots or bars were shown) and the peristimulus time (while the spots and bars were moving) were 1000 ms.

The net firing rate was calculated as the difference between the firing rates during the prestimulus and peristimulus intervals. We defined the net firing rate as the response when a t-test indicated a significant ($p<0.05$) difference between the prestimulus and peristimulus firing rates. To quantify direction selectivity, a direction selectivity index (DI) was calculated, using the formula $DI = 100 \times (R_p - R_{np})/R_p$, where R_p and R_{np} are the net discharge rates of a unit to the stimulus moving in the preferred and non-preferred (opposite) directions, respectively (Dreher et al., 1993).

3.5. Visual stimulation and data analysis to describe the spatio-temporal characteristics of the AEV neurons

For visual stimulation, an 18-inch computer monitor was placed 42.9 cm in front of the animal. The diameter of the stimulation screen was 22.5 cm, so the cat saw it in 30°. To study the spatio-temporal characteristics of the cells, drifting sinusoidal gratings were used. The contrast was constantly 50%. The stimuli were computer-controlled; each of them was presented 12 times in a pseudo-random order. The prestimulus (a stationary sinusoidal grating

was shown) time was 500 ms, as was the peristimulus (a drifting sinusoidal grating was shown) time. The net firing rate was calculated as the difference between the firing rates during the prestimulus and the peristimulus times. We defined the net firing rate as a response when a t-test indicated a significant ($p<0.05$) difference between the two values. To estimate the extent of direction selectivity, DIs were calculated similarly as in the caudate nucleus experiments (Dreher et al., 1993). For each unit tested, sinusoidal gratings were moving along four different axes (0-315° with 45° increments in 8 steps). The preferred directions were used to describe the spatial tuning characteristic of the units. The spatial frequencies were changed between 0.05 and 0.54 cycles/degree (c/deg) with a 0.07 c/deg increment in 8 steps. To examine the temporal characteristic of the units, the stimuli were moved in the preferred directions with the optimal spatial frequency. The temporal frequencies were investigated between 0.6 and 9.6 Hz (cycles/second) in 8 steps.

3.6. Histological control of the recording tracks

At the termination of the experiments, the animals were deeply anesthetized with pentobarbital and were perfused transcardially with 0.9% saline in 0.1 M sodium phosphate buffer (pH 7.4), followed by a mixed solution of 4.0% paraformaldehyde in 0.1 M PBS with 4% sucrose added. The brains were removed and stored overnight in cold buffered 30% sucrose. Frozen coronal sections were cut at 50 μm, mounted immediately and air-dried at room temperature. The coronal sections were stained with neutral red and analyzed under a light microscope.

4. Results

4.1. Receptive field extents of the single AEV neurons

Altogether 150 cells were recorded that were sensitive to either visual or auditory stimulation or both. Upon comparison of the peristimulus discharge rate with the prestimulus discharge rate, visual sensitivity was found in 59 cells. Sixty cells were found to be auditory-sensitive, while 31 cells proved to be bimodal in the sense that they reacted to separate visual and separate auditory stimulation, and also to simultaneous auditory and visual stimulation to a statistically significant extent.

4.1.1. Subjective estimation of the receptive field extents

Both visual and auditory cells possess extremely large receptive fields. Since our stimulating set was confined to 165°, which was smaller than the auditory receptive field defined earlier (Midlebrooks et al., 1994; 1998), we did not attempt to delineate the total extents of the auditory receptive fields. Subjective estimation of the visual receptive field indicated in all cases that it covered a major part of the contralateral hemifield and extended deep into the ipsilateral one, yielding a field that overlapped almost totally with the visual field of the right eye. No signs of retinotopy were observed within the AEV.

4.1.2. Objective estimation of the visual, auditory and bimodal receptive field extents

Objective estimation of the visual, auditory and bimodal receptive fields was performed by calculating the significant responses to individual stimulation given at a distance of 15° with the help of the t-test. The width of the receptive field of a neuron was determined by the locations of stimuli that induced a significant response. This procedure obviously underestimates the actual size of the receptive field, but it yields an objective estimate that can be used in further analysis (Fig. 2).

The mean extent of the visual receptive fields in the horizontal plane was obtained as 75.8° (N=59; SD: ±28.6°; range: 15-135°; Fig. 3A). Nevertheless, only 4 visual cells revealed significant responses in the whole extent of the 135° field (the visual field of the right eye) studied, in most cases since the peripheral parts of the receptive fields rarely displayed

significantly increased responses. The site of maximal responsivity within the visual receptive fields varied extensively in the cells recorded. The visual field did not appear to contain any exclusive site consistently preferred by a majority of the cells. Practically all the stimulating sites produced a maximal response in some cells, while other cells had a preference for other sites (Fig. 4). We compared the PSTHs obtained upon ipsilateral and contralateral visual stimulation. ANOVA analysis of the net firing rates yielded significant differences between these responses in 42.4% (25 of 59) of the visual cells.

The mean extent of the auditory receptive fields in the horizontal plane, as estimated statistically, was found to be 132.5° (N=60; SD: ±46.7°; range: 15-165°; Fig. 3B) in the 165° perimeter examined. Thirty-two auditory cells displayed receptive fields extending to the 165° area studied. The different auditory neurons (similarly to the visual ones) responded maximally to stimulations coming from different stimulus locations (Fig. 5). No signs of laterality were observed in the auditory cells. The comparison of PSTHs recorded upon ipsilateral and contralateral auditory stimulation indicated only weak, nonsignificant differences.

The mean bimodal receptive field extent of the bimodal cells in the horizontal plane was 82.1° (N=31; SD: ± 22.2°; range: 30-135°; Fig. 3C). The site of maximal response to combined stimulation varied extensively within the receptive fields of the bimodal neurons (Fig. 6). No signs of laterality were detected upon ipsilateral and contralateral bimodal stimulation of the bimodal cells.

4.1.3. Extent of facilitatory cross-modal interactions

We analyzed the receptive field data for the 21 bimodal neurons that exhibited a significant facilitatory cross-modal interaction between visual and auditory stimulation. The mean extent of the facilitatory interaction in these cells was 75.7° (N=21; SD: ±24.6°; range: 45-135°). We failed to find any site-relatedness of the cross-modal interaction within the perimeter studied. The relationship between the cross-modal facilitation calculated by the formula of Meredith & Stein (1986) and the stimulation site was found by ANOVA to be statistically non significant ($F(9,190)=0.619$, $p=0.78$).

4.2. Visual receptive field properties of single neurons in the caudate nucleus

4.2.1. Distribution of the visual neurons in the caudate body

Altogether 157 single neurons were recorded in the caudate nucleus. Fifty-four of these units (34.4%) showed visual sensitivity. The response and receptive field properties of these 54 visually responsive neurons were analyzed. As can be seen from the histological reconstruction of the recording tracks shown in Fig. 7, the distribution of these visually responsive neurons was essentially confined to the body of the caudate nucleus. Most of the recorded units were located between the Horsley-Clark co-ordinates anterior 12 and 13 and lateral 4 and 6.5, although some visual units were recorded at anterior 14 and 15, too. Visually responsive units were confined to the dorsolateral part of the caudate nucleus. We could not detect visual responsive caudate nucleus units in its more anterior part (anterior 16 and 17).

4.2.2. Receptive field extent of the caudate nucleus units

The visual sensitive units showed a preference for stimuli moving at a considerable speed (30 deg/s or higher). The responsivity of the neurons to static visual stimulation was much lower. From this fact, the detection of the exact borders of the receptive fields was not easy. Subjective estimation of the visual receptive fields was performed by listening to the responses to movements of a hand-held lamp. The receptive fields were extremely large: they seemed to contain most of the contralateral visual hemifield and additionally a major part of the ipsilateral hemifield. The receptive fields consistently included the area centralis. No signs of retinotopy were observed.

4.2.3. Direction selectivity and direction tuning of the caudate neurons

Small spots 1° in diameter moving sequentially in 8 different directions (moving with optimal velocity for each unit) were used to determine the optimal direction of the units. Within the population of visually responsive neurons, the optimal direction varied extensively. The preference for the optimal directions was distributed almost uniformly among the neurons.

Direction tuning widths were analyzed in 54 neurons. The tuning width was defined as the range of directions over which the firing rate was at least half the maximal one. Twenty-

nine units (53.7%) showed significant responses to only one direction of stimulus movement. This means that their tuning width was less than 45°. Another 19 units (35.2%) were narrowly tuned: their tuning widths were either 45° or 90°. The remaining 6 cells (11.1%) exhibited broad directional tuning characterized by a 180-360° tuning width.

The directional sensitivity of the 54 cells was calculated by using the DIs (Dreher et al., 1993). Thirty-two of the units (59.3%) were direction-selective: they exhibited a DI of >90%. In 24 cases, even an inhibition of the spontaneous activity was detected in the direction opposite to the preferred one (Fig. 8B). Six cells (11.1%) were direction-sensitive as they gave a DI of between 50% and 90%. It is noteworthy that 16 units (29.6%) were not direction-sensitive: they furnished a DI of <50% (Fig. 8A). This group contained the 6 broadly-tuned units.

4.2.4. Velocity tuning and stimulus size preferences of the caudate nucleus neurons

Small spots 1° in diameter moving in the optimal direction for each unit were used to determine the velocity tuning function of the caudate nucleus neurons. Each unit was tested with four different velocities (15, 30, 60 and 120 deg/s) to estimate their velocity preference. The caudate units evidently preferred intermediate or high velocities. Thirty-two of the 54 neurons (59.2%) were most responsive to 60 deg/s, while 11 units each (20.4%) elicited the most vigorous responses to either 30 deg/s or 120 deg/s. None of the caudate nucleus units displayed optimal responsivity to the lowest examined velocity (15 deg/s). In summary, 43 of the 54 neurons demonstrated band-pass tuning characteristics under our stimulation conditions. These cells had a clear optimal velocity. Both below and above this velocity, the responsivity of these neurons was attenuated. The remaining 11 units could be considered high-pass tuned ones. They showed attenuation at all velocities below the highest velocity tested.

Fifty-four cells were tested with moving light bars of four different sizes, 1° x 1°, 1° x 3°, 1° x 5° and 1° x 10°, to determine their stimulus size preferences. The bars were moved in the optimal direction with optimal velocity in each case. Altogether 68.6% of the cells (37/54) responded preferentially to the smallest, "spot-like" (1° x 1°) stimulus. A small proportion of the cells responded optimally to stimuli of larger size. Three neurons (5.5%) gave a maximal response to the 1° x 3° and 1° x 5° bars, while 4 of them (7.4%) were most responsive to the 1° x 10° stimuli. Seven of the 54 (13.0%) units were not sensitive to the length of the stimuli. They yielded almost the same net firing rate for all stimulus lengths tested.

4.3. Spatial and temporal visual properties of neurons in the AEV

4.3.1. Direction selectivity and direction tuning function of the cells

Recordings obtained in 75 single-units in the AEV were evaluated. Sinusoidal gratings drifting consecutively in 8 different directions (4 different axes of movement) were used to determine the optimal direction of each unit. The distribution of the preferred directions of the 75 single-units recorded in the AEV is shown in Fig. 9A. It is apparent that very few cells (7/75; 9.3% of the sample) exhibited preferences for movement along horizontal axis (90° and 270° directions). Preference for the remainder of the directions was common among the neurons.

The direction tuning widths of these 75 AEV units were analyzed in detail. The tuning width was defined as the range of directions over which the firing rate was at least half the maximal one. Forty-five units (60.0%) showed significant responses to only one direction of stimulus movement. This means that their tuning width was less than 45°. Another 20 units (26.7%) were narrowly tuned: their tuning widths were either 45° or 90°. The remaining 10 cells (13.3%) exhibited broad directional tuning characterized by a 135-270° tuning width.

The direction sensitivity of the cells was calculated by using the DI adopted from Dreher et al. (1993) (Fig. 9B). Thirty-nine of the units (52.0%) exhibited a DI >90%, i.e.these neurons are very strongly direction-selective and their responses are greatly attenuated for the opposite direction. For 25 of these 39 strongly direction-selective single neurons, even inhibition of the spontaneous activity was detected in the direction opposite to the preferred one. It is noteworthy that only 8 units (10.7%) exhibited a DI of <50%. The remaining 28 units (37.3%) exhibited DIs in the interval 50-90%.

4.3.2 Spatial frequency tuning and spatial bandwidths of the AEV units

The spatial frequency tuning function of the AEV neurons was determined on the basis of their responses to drifting sinusoidal gratings moving in the optimal direction. All the cells displayed responses to rather low spatial frequencies (Fig. 10A shows the responses of a typical AEV single cell to different spatial frequencies); a maximal response could not be recorded for any of them at spatial frequencies >0.47 c/deg (Fig. 11D). Spatial frequencies above 0.47 c/deg caused inhibition of the spontaneous activity in 23 units. Most of the cells (69/75; 92.0%) demonstrated band-pass characteristics, as illustrated by the representative

examples in Fig. 11A, B. These cells had a clear optimal spatial frequency; above and below this spatial frequency, the discharge rate was lower. Only 6 of the 75 neurons (8.0%) exhibited low-pass characteristics under the present stimulating conditions, with no attenuation of the response for the low spatial frequencies. Fig. 11C shows a typical low-pass unit. The optimal spatial frequency of the AEV neurons was observed in the range 0.13-0.47 c/deg, with a mean at 0.20 c/deg (N=75; SD: ±0.08 c/deg).

The spatial bandwidths of 34 band-pass units were analyzed (Fig. 11E). The spatial bandwidth was measured at the half-height of the spatial frequency-tuning curve. This indicates the spatial selectivity of the cell. Most of the AEV single neurons were narrowly tuned to spatial frequencies. The mean spatial bandwidth was 1.4 octaves (N=34; SD: ±0.7 octaves; range: 0.3-3.0 octaves). Some cells, however, were broadly tuned. Five of the 34 neurons revealed a spatial bandwidth >2 octaves.

4.3.3. Temporal frequency tuning and temporal bandwidths of the AEV cells

Sinusoidal gratings of optimal spatial frequency and moving in the optimal direction were applied to evaluate the temporal frequency tuning of the neurons. Most of the cells displayed responses to rather high temporal frequencies. Fig.10B shows the responses of a typical AEV single cell to different temporal frequencies. Three kinds of temporal tuning functions were apparent under the present stimulating conditions: high-pass (23/75; 30.7%), band-pass (50/75; 66.7%) and low-pass (2/75; 2.6%). Fig. 12A depicts a typical band-pass unit with a clear optimal temporal frequency. High-pass cells responded optimally to the highest temporal frequency tested (Fig. 12B). Low-pass cells exhibited the maximal response to the lowest temporal frequency tested; higher temporal frequencies resulted in weaker responses (Fig. 12C). Overall, a majority of the units responded maximally to high temporal frequencies with a mean at 6.3 Hz (N=75; SD: ±2.3 Hz; range: 0.6-10.8 Hz), although we also found cells with preferences for all examined temporal frequencies (Fig. 12D).

The temporal bandwidth, defined as the range of temporal frequencies over which the responses were at least half of the maximal one, was determined for 46 of the 50 band-pass units. This indicates the temporal selectivity of the cell. The cells were narrowly tuned to temporal frequencies. The mean temporal bandwidth was 1.1 octaves (N=46; SD: ±0.5 octaves; range: 0.2-3.5 octaves), (Fig. 12E).

5. Discussion

5.1. Visual, auditory and bimodal receptive field extent of the AEV neurons

Our results add new data to the multimodal representation of the environment in the feline cortex. Detailed analyses of the visual, somatosensory and auditory properties of the AEV neurons and their cross-modal interaction were performed earlier (Hicks et al., 1988a; Wallace et al., 1992; Stein & Wallace, 1996). Our results on the existence of visual or auditory unimodal cells, together with bimodal cells that show a cross-modal interaction, appear to be entirely in line with these earlier results. Despite all these studies, an exact estimation of the visual receptive field extent is still missing. Even the existence of retinotopy in this area is a matter of controversy (Olson & Graybiel, 1987; Benedek et al., 1988; Scannel et al., 1996). Our subjective estimations demonstrated extremely large visual receptive fields that cover the visual field of the investigated eye. We did not observe any signs of retinotopy within the AEV. Our novel, objectively estimated, statistical approach confirmed the earlier observation by our group (Benedek et al., 1988) that a large number of the AEV neurons have very large receptive fields that cover most of the whole visual field of the corresponding eye. The stimulation pattern used in our experiments was selected because some neurons were insensitive to diffuse on-off light stimulation. However, in some cases our objectively estimated receptive field sizes are much smaller. The reason for this may be that the stimuli were not optimal for all of the recorded neurons and thus the receptive field sizes may be underrepresented in our sample. The different visual neurons possess sites of maximal sensitivity to different regions of their large receptive field. No exclusive site was found that was preferred by a majority of the visual units.

Similarly as in earlier reports (Middlebrooks et al., 1994; 1998; 2002), the auditory receptive fields were found to be extremely large. Since our stimulating set was confined to the anterior 165° of a horizontal plane, the area of which is much smaller than the auditory receptive field defined earlier, we did not attempt to delineate the total extent of the auditory receptive fields. Nevertheless, in most neurons the auditory receptive field covered the whole of the area we studied. The different auditory neurons possess sites of maximal sensitivity to different regions of their large receptive field.

Objective estimation showed that the bimodal receptive fields are also extremely large. In most cases, the bimodal receptive fields of the bimodal neurons extended to the borders of the visual field of the right eye, although their auditory receptive fields were somewhat larger.

Similarly to the visual and auditory neurons, the different bimodal neurons possess sites of maximal sensitivity to different regions of their receptive field.

In the experiments reported here, 21 bimodal neurons displayed significant multisensory cross-modal facilitation. The extent of the bimodal facilitatory interactions was found to be similar to that of the visual receptive fields. We did not observe any relationship between the strength of the interactions calculated with the formula of Meredith & Stein (1986) and the stimulation site.

5.2. Visual receptive field properties of the caudate nucleus single neurons

Visual activity in the caudate nucleus has been reported by several laboratories (Pouderoux & Freton, 1979; Rolls et al., 1983; Strecker et al., 1985; Hikosaka et al., 1989; Kolomiets, 1993; Brown et al., 1995), but we have given the first description of the receptive field properties of visual single neurons in the feline caudate nucleus. Our results are novel from the aspect that we could record visual neuronal activity in the caudate nucleus of the brain in anesthetized, paralyzed cats, which allowed an exact determination of the visual receptive field properties. We found visual neuronal activity in the dorsolateral part of the caudate nucleus. This region corresponds fully to that reported to receive afferentation from both the extrageniculate visual cortical areas and the extrageniculate visual thalamus (Niida et al., 1997; Harting et al., 2001a, b; McHaffie et al., 2001).

The receptive field of the caudate nucleus units is extremely large, covering most of the contralateral and the ipsilateral visual hemifields and consistently including the area centralis. Earlier physiological experiments on animals under chloralose anesthesia (Pouderoux & Freton, 1979) indicated the existence of large receptive fields. Neurons in the intermediate and deep layers of the SC similarly display large receptive fields that often extend into the ipsilateral hemifield (Wallace & Stein, 1996). The receptive fields of caudate neurons most closely resemble those found in the neurons of the feline extrageniculate thalamus, e.g. the LM-Sg (Benedek et al., 1996) and those of the cortex along the anterior ectosylvian sulcus (Benedek et al., 1988; Benedek & Hicks, 1988). The lateral suprasylvian areas and other extrastriatal visual areas that project to the caudate nucleus similarly possess large receptive fields (Spear, 1991; Sherk & Mulligan, 1992).

Directionally sensitive units were previously not detected within the caudate nucleus (Pouderoux & Freton, 1979). We have observed two general classes of directional tuning sensitivity within the caudate single neurons. A majority of the cells display narrow

directional tuning and high direction selectivity. A smaller proportion of the units exhibits broad directional tuning. Although directionally sensitivity is an inherent property of the neurons in the striatal cortex (Hammond & Andrews, 1978), the highest level of directional sensitivity has been reported in the neurons of the SC (Sterling & Wickelgren, 1969) and those in its thalamo-cortical projection (Benedek & Hicks, 1988; Benedek et al., 1988; 1996). The directional tuning of the caudate neurons revealed by our results seems to be rather sharp as compared with the striatal or extrastriatal visual areas of the cat (Henry et al., 1974; Hammond & Andrews, 1978; von Grünau & Frost, 1983; Benedek et al., 1988; Benedek & Hicks, 1988).

The caudate nucleus units prefer intermediate or high velocities, but not low velocities, and most of them show band-pass velocity tuning characteristic. A majority of the units prefer a small spot-like moving stimulus and their responsivity is highly attenuated for larger sizes. This preference of caudate neurons for small stimuli moving at higher velocities is similar to that of SC neurons (Wang et al., 2001) and also those in the thalamic (LM-Sg) and cortical regions (AEV and IVA) that receive strong tectal afferents (Mucke et al., 1982; Benedek & Hicks, 1988; Benedek et al., 1988; 1996).

5.3. Spatio-temporal characteristics of the AEV neurons

The electrophysiological studies that described the AEV in the cat were essentially limited to defining its optimal spatial and temporal visual properties. The only related study that dealt with square-wave stimulation led to the conclusion that the single cells in this specific area were responsive to low spatial and high temporal frequencies (Hicks et al., 1988). Responses to drifting sinusoidal grating stimuli have never been investigated before. The aims of our investigations were to examine the spatial and temporal properties of the AEV neurons by using drifting sinusoidal grating stimuli, and to compare these properties with those described for other visual areas in order to acquire a better understanding of the possible role that the AEV plays in visual information processing.

More than 50% of the AEV units displayed DIs >90%. These units were clearly selective as concerns the stimulus direction. Previous studies in which the AEV was stimulated with simple geometric forms similarly suggested a high proportion of direction-selective units in the AEV (Mucke et al., 1982; Benedek et al., 1988; Hicks et al., 1988b). Direction-selective cells are also common in areas 17 (Hammond & Andrews, 1978), 18 (Rose & Blakemore, 1974), 21b (Tardif et. al., 2000) and in the PMLS area (Blakemore &

Zumbroich, 1987), but less common in areas 19 (Bergeron et al., 1998) and 21a (Wimborne & Henry, 1992; Dreher et al., 1993; Tardif et al., 1996). It seems that the AEV has a higher proportion of strongly direction-selective cells than any of the other visual cortical areas. The high proportion of directional-selective neurons in the AEV resembles that in the retino-recipient layers of the SC (Sterling & Wicklegren, 1969; Dreher & Hoffmann, 1973). The inhibition of spontaneous activity in the direction opposite to the optimal one was a characteristic feature of one third of the investigated AEV units. This suppression is often a characteristic feature of cells in area 21b (Tardif et al., 2000) and cells in the retino-recipient, deep layers of the SC (Dreher & Hoffman, 1973). Interestingly, the deep layers of the SC (but not the superficial layers) receive a strong afferentation from the AEV and send heavy efferents to the LM-Sg complex of the visual thalamus (Harting et al., 1992). Most of the AEV neurons are narowly tuned to the stimulus direction, although we could record some broadly tuned neurons too.

The AEV units responded well to drifting gratings and clearly preferred low spatial frequencies. Most of the units exhibit band-pass characteristics, though some low-pass cells were also recorded. These two types of spatial frequency tuning were also observed in cells recorded in areas 17 (Ikeda & Wright, 1975), 18 (Movshon et al., 1978), 19 (Bergeron et al., 1998), 21a (Tardif et al., 1996), 21b (Tardif et al., 2000) and the PMLS area (Zumbroich & Blakemore, 1987). The mean optimal spatial frequency of the AEV cells is 0.20 c/deg. This is similar to the mean values for some other extrastriate visual areas, such as area 18 (0.22 c/deg; Movshon et al., 1978), area 19 (0.17 c/deg; Tardif et al., 1997; Bergeron et al., 1998), area 21a (0.36 c/deg; Tardif et al., 1996.), area 21b (0.08 c/deg; Tardif et al., 2000) and the PMLS area (0.16 c/deg; Zumbroich & Blakemore, 1987). In area 17, the mean optimal spatial frequencies are considerably higher: 0.86 c/deg and 0.93 c/deg for simple and complex cells, respectively (Movshon et al., 1978). This is possibly due to a strong X signal from the geniculate nucleus to area 17, which carries high spatial frequency information. The SC units respond optimally to low spatial frequencies in the interval 0.05-0.1 c/deg (Pinter & Harris, 1981), a level, which is slightly lower than the optimal for most AEV units.

The mean spatial bandwidth of the cells in the AEV is 1.4 octaves. This means that the AEV units are narrowly tuned and may suggest that they are good spatial filters. This mean value is similar to the mean spatial bandwidths for areas 17 (1.5 octaves; Movshon et al., 1978), 18 (1.49 octaves; Movshon et al., 1978) and 21a (1.6 octaves; Tardif et al., 1996), but differs from those for areas 19 (1.9 octaves; Tanaka et al., 1987), 21b (2.2 octaves; Tardif et al., 2000) and the PMLS area (2.2 octaves; Zumbroich & Blakemore, 1987). The cells in the

SC, like the AEV units, are also sharply tuned to low spatial frequencies (Pinter & Harris, 1981).

The temporal frequency tuning functions of the neurons in the AEV are mainly band-pass, rarely high-pass and only in 2 cases low-pass. A big majority of the units responded optimally to high temporal frequencies over 4 Hz. The mean optimal temporal frequency of the AEV cells is 6.3 Hz. This is the second highest mean optimal temporal frequency for the feline visual cortical areas that have so far been investigated. It is comparable to the mean value for area 21a (around 7 Hz; Tardif et al., 1996), but much higher than the mean value for other visual cortical areas: areas 17 (2.9 Hz; Saul & Humphrey, 1992), 18 (3.2 Hz; Saul & Humphrey, 1992), 19 (3 Hz; Bergeron et al., 1998), 21b (3.2 Hz; Tardif et al., 2000) and the PMLS area (5 Hz; Morrone et al., 1986). The cells in the AEV have mean temporal frequencies resembling that of the SC: 6.4 Hz (Pinter & Harris, 1981).

The mean temporal bandwidth of the neurons in the AEV is 1.1 octaves. This is the smallest tuning width for all feline visual cortical areas tested so far, e.g. areas 17 (1.7 octaves; Movshon et al., 1978), 18 (1.5 octaves; Movshon et al., 1978), 19 (2.9 octaves; Bergeron et al., 1998), 21a (2.9 octaves; Tardif et al., 1996), 21b (3.3 octaves; Tardif et al., 2000) and the PMLS area (about 2 octaves; Morrone et al., 1986). The AEV cells seem to be the most narrowly tuned units to temporal frequencies in the feline visual cortex, and hence they could be very good temporal filters. Similarly to the AEV neurons, the SC units are also sharply tuned to high temporal frequencies (Pinter & Harris, 1981).

In summary, we can conclude that the AEV neurons prefer low spatial and high temporal frequencies and these units display narrow spatial and temporal tuning characteristics. Earlier studies with square-wave stimulation (Hicks et al., 1988b) failed to reveal these fine tuning properties. The low spatial frequency and high velocity preference of the cells in the AEV suggest that they receive strong Y signals presumably through the tecto-suprageniculate route (Benedek et al., 1996) or from the PMLS area, either directly or via the relay in the LPm region of the thalamus (for a review, see Dreher, 1986). This corroborates well with the findings of Wang et al. (1998), who concluded that the AEV units are dominated by Y inputs.

It is worth speculating about the functional role of the AEV in the knowledge of the particular physiological properties of the AEV neurons. Tamai et al. (1989) observed that intracortical microstimulation of the AEV evoked centering movements of both eyes. They suggested that the AEV might be involved in the control of eye movements. As mentioned earlier, the AEV projects strongly to the deep layers of the ipsilateral SC (Harting et al. 1992).

The SC in turn, and especially the deep layers, play an important role in visual guided eye movements (for a review, see Stein & Meredith 1991). Our results suggest another possible functional role of the AEV, as it can also be involved in motion perception. In human vision, the motion detectors extend over a wide range of spatial frequencies, but do not seem to be prevalent at high spatial frequencies (Anderson & Burr, 1985). All motion detectors are apparently finely tuned for temporal and spatial frequencies (Anderson & Burr, 1985), the narrow tuning aiding the velocity detection and the analysis of the object in motion (Burr & Ross, 1986; Burr et al., 1986). Neurons in the PMLS area that similarly respond optimally to low spatial frequencies and high temporal frequencies and are relatively narrowly tuned to spatial and temporal frequencies (Morrone et al., 1986) are involved in the optic flow processing (Brosseau-Lachaine et al., 2001). We suggest that the AEV neurons with preferences for low spatial frequencies and with their fine spatial and temporal tuning may have a function similar to that in the PMLS area. Since these neurons have the capacity to perceive optic flow, they could be good candidates for tasks involved in the perception of self-motion. We suggest that the AEV may play a role in the recording of movements of the visual environment relative to the body and thus it may participate in the adjustment of motor behavior in response to environmental challenges.

6. Conclusions

The visual, auditory and bimodal neurons along the AES have extremely large receptive fields. Any single neuron in the AEV that receives appropriate modality sensory stimulation can carry information from stimuli within its whole physically approachable sensory field. The different neurons possess sites of maximal sensitivity to different regions of their large receptive fields. No signs of retinotopy were observed within the AEV. The absence of traditional topographic coding raised the idea that there could be a peculiar type of spatial coding in the extrageniculate tecto-thalamo-cortical visual system. Our observations suggest the existence of distributed population coding for the visual, auditory and bimodal stimulus source localization in the extrageniculate visual system.

Our results demonstrate that the caudate nucleus units possess particular visual receptive field properties that show similarities to those of the SC neurons and also those in thalamic and cortical regions that receive strong tectal afferents (LM-Sg, AEV and IVA). Thus, the earlier-described tecto-thalamo-cortical visual system extends toward the caudate nucleus, which receives its visual afferentation from the SC through the LM-Sg complex of the visual thalamus.

The neurons in the extrageniculate visual system respond optimally to moving visual stimuli. Their responsivity to stationary stimulation is much weaker. These neurons seem to be novelty detectors. Our results that describe the spatio-temporal visual characteristics of the AEV suggest a special behavioral role of the extrageniculate visual system. The narrow spatial and temporal tuning might contribute to velocity detection and to the analysis of the object in motion. The extrageniculate visual system may be involved in the optic flow processing and could be a good candidate for tasks involved in the perception of self-motion. We suggest that the AEV may play a role in the recording of movements of the visual environment relative to the body and thus it may participate in the adjustment of motor behavior in response to environmental challenges.

In summary, our results add new data to the multimodal representation of the environment in the mammalian brain, extend the earlier-described tecto-thalamo-cortical extrageniculate visual system toward the caudate nucleus and help to clarify the functional role of the extrageniculate visual system of the mammalian brain.

7. Summary

Electrophysiological recording of single units in the AEV and the caudate nucleus was carried out extracellularly via tungsten microelectrodes in halothane-anesthetized, immobilized, artificially respirated cats. Neuronal activities were recorded and correlated with the movement of the light stimulus by a computer and stored for further analysis as PSTHs. The net firing rate was calculated as the difference between the firing rates during the prestimulus and peristimulus intervals. The net firing rate was defined as a response when a t-test revealed a significant ($p<0.05$) difference between the two values. Vertical penetrations were performed between the Horsley-Clarke co-ordinates anterior 12-17 and lateral 4-6.5 in the stereotaxic depths in the interval 12-19 to record caudate nucleus neurons, and anterior 10-14 and lateral 12-14 in the stereotaxic depths in the interval 13-17 to record the AEV neurons.

To estimate the extents of the visual, auditory and bimodal receptive fields of the AEV neurons, we introduced a quasi-objective computer-controlled method. The receptive field extents were estimated by calculating the significant responses to individual stimulation given at a distance of 15°, with the help of the t-test. The width of the receptive field of a neuron was determined by the locations of stimuli that induced a significant response. The mean extent of the visual receptive fields in the horizontal plane was obtained as 75.8° (N=59; SD: ±28.6°; range: 15-135°). Nevertheless, only 4 visual cells revealed significant responses in the whole extent of the 135° field (the visual field of the right eye) studied, in most cases since the peripheral parts of the receptive fields rarely displayed significantly increased responses. The site of maximal responsivity within the visual receptive fields varied extensively in the cells recorded. The visual field did not appear to contain any exclusive site consistently preferred by a majority of the cells. Practically all the stimulating sites produced a maximal response in some cells, while other cells had a preference for other sites. The mean extent of the auditory receptive fields in the horizontal plane, as estimated statistically, was found to be 132.5° (N=60; SD: ±46.7°; range: 15-165°) in the 165° perimeter examined. Thirty-two auditory cells displayed receptive fields extending to the 165° area studied. The different auditory neurons (similarly to the visual ones) responded maximally to stimulations coming from different stimulus locations. The mean bimodal receptive field extent of the bimodal cells in the horizontal plane was 82.1° (N=31; SD: ± 22.2 °; range: 30-135°). The site of maximal response to combined stimulation varied extensively within the receptive fields of the bimodal neurons. We analyzed the receptive field data for the 21 bimodal neurons that exhibited a significant facilitatory cross-modal interaction between visual and auditory stimulations. The

mean extent of the facilitatory interaction in these cells was 75.7° (N=21; SD: ±24.6°; range: 45-135°). We did not observe any relationship between the strength of the interactions calculated with the formula of Meredith and Stein (1986) and the stimulation site. The visual, auditory and bimodal neurons along the AES have extremely large receptive fields. Any single neuron in the AEV that receives appropriate modality sensory stimulation can carry information from stimuli within its whole physically approachable sensory field. The different neurons possess sites of maximal sensitivity to different regions of their large receptive fields. The absence of traditional topographic coding gave rise to the idea that there could be another type of spatial coding in the tecto-thalamo-cortical extrageniculate visual system. Our observations suggest the existence of distributed population coding for the visual, auditory and bimodal stimulus source localization in the extrageniculate visual system.

The most noteworthy findings of our work were the recording of visual active neurons in the feline caudate nucleus and the description of the visual receptive field properties of the single caudate neurons. Visually responsive units were confined to the dorsolateral part of the caudate nucleus. Most of the recorded units were located between the Horsley-Clark co-ordinates anterior 12 and 13 and lateral 4 and 6.5, although some visual units were recorded at anterior 14 and 15, too. We could not detect visual responsive caudate nucleus units in its more anterior part (anterior 16 and 17). The visual sensitive units showed a preference for stimuli moving at a considerable speed (30 deg/s or higher). The responsivity of the neurons to static visual stimulation was much lower. The receptive fields were extremely large: they seemed to contain most of the contralateral visual hemifield and additionally a major part of the ipsilateral hemifield. The receptive fields consistently included the area centralis. No signs of retinotopy were observed. Most of the neurons are narrowly tuned to the stimulus direction and direction-selective. However, a smaller proportion of the caudate units exhibited broad direction tuning and was not directions-sensitive. The caudate nucleus units responded optimally to small, spot-like stimuli moving with intermediate or high velocities. Our results demonstrate that the caudate nucleus units possess particular visual receptive field properties that show strong similarities to those of the SC neurons and also those in thalamic and cortical regions that receive strong tectal afferents (LM-Sg, AEV and IVA) and differ considerably from those of the geniculo-striatal visual system. Thus the earlier-described tecto-thalamo-cortical visual system extends toward the caudate nucleus, which receives its visual afferentation from the SC through the LM-Sg complex of the visual thalamus.

We have further investigated the spatio-temporal visual properties of the single neurons in the feline visual associative cortex. The AEV neurons were strongly selective to

the direction of the drifting gratings. Most of the cells (69/75; 92.0%) demonstrated band-pass spatial tuning characteristics. Six of the 75 neurons (8.0%) exhibited low-pass spatial tuning characteristics. The optimal spatial frequency of the AEV units was observed in the range 0.13-0.47 c/deg, with a mean at 0.20 c/deg (N=75; SD: ±0.08 c/deg). Most of the AEV single neurons were narrowly tuned to spatial frequencies. The mean spatial bandwidth was 1.4 octaves (N=34; SD: ±0.7 octaves; range: 0.3-3.0 octaves). Three kinds of temporal tuning functions were apparent under the present stimulating conditions: high-pass (23/75; 30.7%), band-pass (50/75; 66.7%) and low-pass (2/75; 2.6%). Most of the cells displayed responses to rather high temporal frequencies with a mean at 6.3 Hz (N=75; SD: ±2.3 Hz; range: 0.6-10.8 Hz,). The mean temporal bandwidth was 1.1 octaves (N=46; SD: ±0.5 octaves; range: 0.2-3.5 octaves). This is the smallest tuning width for all feline visual cortical areas tested so far. It seems that the AEV neurons are the most narrowly tuned visual units to temporal frequencies in the feline brain. This fine spatial and temporal tuning characteristic of the AEV neuron suggests that they are good spatial and temporal filters. The neurons in the extrageniculate visual system respond optimally to moving visual stimuli. Their responsivity to stationary stimulation is much lower. These neurons seem to be novelty detectors. Our results that describe the spatio-temporal visual characteristics of the AEV suggest a special behavioral role of the extrageniculate visual system. The narrowly spatial and temporal tuning aids the velocity detection and the analysis of the object in motion. The extrageniculate visual system may be involved in the optic flow processing and could be a good candidate for tasks involved in the perception of self-motion. We suggest that the AEV may play a role in the recording of movements of the visual environment relative to the body and thus it may participate in the adjustment of motor behavior in response to environmental challenges.

In summary, our results add new data to the multimodal representation of the environment in the mammalian brain, extend the extrageniculate visual system to the caudate nucleus and can help to clarify the functional role of the extrageniculate visual system of the mammalian brain.

8. Acknowledgments

I greatly appreciate the extremely helpful and instructive guidance of my professor and supervisor Dr. György Benedek. I wish to express my deepest thanks to my colleague and wife, Gabriella Eördegh, for her continuous love, encouragement, comfort and aid in my work and in my life. I express my most sincere gratitude to Gabriella Dósai for her valuable technical assistance and for the preparation of high-quality figures for my dissertation. Many thanks are due to Péter Liszli for his expert help in solving hardware and software problems. I would like to acknowledge the help of Zita Márkus, Alíz Roxine and Antal Berényi in the data collection. I express my gratitude to Dr. Zoltán. Chadaide, Károly Köteles, Dr. Gyula Sáry and Tamás Tompa my direct colleagues in the Visual Laboratory for their help and friendship. I would like to express my deepest thanks to all colleagues in the Department of Physiology for their support. It was good to work with them in that department.

My deepest thanks are due to my family for their continuous love and help in my life.

Our experiments were supported by OTKA/Hungary grant 29817, OTKA/Hungary grant T42610 and FKFP/Hungary grant 0455/2000.

9. References

Anderson SJ, Burr DC (1985) Spatial and temporal selectivity of the human motion detection system. Vision Res 25:1147-1154

Benedek G, Fischer-Szatmári L, Kovács G, Perényi J, Katoh YY (1996) Visual, somatosensory and auditory modality properties along the feline suprageniculate-anterior ectosylvian sulcus/insular pathway. Prog Brain Res 112:325-334

Benedek G, Hicks TP (1988) The visual insular cortex of the cat: organization, properties and modality specificity. Prog Brain Res 75:271-278

Benedek G, Jang EK, Hicks TP (1986) Physiological properties of visually responsive neurones in the insular cortex of the cat. Neurosci Lett 64:269-274

Benedek G, Mucke L, Norita M, Albowitz B, Creutzfeldt OD (1988) Anterior ectosylvian visual area (AEV) of the cat: physiological properties. Prog Brain Res 75:245-255

Benedek G, Perény J, Kovács G, Fischer-Szatmári L, Katoh YY (1997) Visual, somatosensory, auditory and nociceptive modality properties in the feline suprageniculate nucleus. Neuroscience 78:179-189

Benedek G, Sztriha L, Kovács G (2000) Coding of spatial co-ordinates on neurones of the feline visual association cortex. Neuroreport 11:1-4

Bergeron A, Tardif E, Lepore F, Guillemot JP (1998) Spatial and temporal matching of receptive field properties of binocular cells in area 19 of the cat. Neuroscience 86:121-134

Blakemore C, Zumbroich TJ (1987) Stimulus selectivity and functional organization in the lateral suprasylvian visual cortex of the cat. J Physiol 389:569-603

Brosseau-Lachaine O, Faubert J, Casanova C (2001) Functional sub-regions for optic flow processing in the posteromedial lateral suprasylvian cortex of the cat. Cereb Cortex 11:989-1001

Brown VJ, Desimone R, Mishkin M (1995) Responses of cells in the tail of the caudate nucleus during visual discrimination learning. J Neurophysiol 74:1083-1094

Burr DC, Ross J (1986) Visual processing of motion. Trends in Neurosci 9:304-307

Burr DC, Ross J, Morrone M (1986) Seeing objects in motion. Proc Roy Soc Lond B227:249-265

Comoli E, Coizet V, Canteras NS, Westby GWM, Redgrave P (2001) Direct projection from superior colliculus to dopaminergic neurons in the ventral midbrain. Soc Neurosci Abstr 27:68.11

Dreher B (1986) Thalamocortical and coricocortical interconnections in the cat visual system: relation to the mechanisms of information processing. In:Pettigrev JD, Sanderson KJ, Levick WR (eds) Visual Neuroscience, Cambridge University Press, Cambridge, pp 290-317

Dreher B, Hoffmann KP (1973) Properties of excitatory and inhibitory regions in the receptive fields of single units in the cat's superior colliculus. Exp Brain Res 16:333-353

Dreher B, Michalski A, Ho RH, Lee CW, Burke W (1993) Processing of form and motion in area 21a of cat visual cortex. Vis Neurosci 10:93-115

Hammond P, Andrews DP (1978) Orientation tuning of cells in areas 17 and 18 of the cat's visual cortex. Exp Brain Res 31:341-351

Hardy H, Heimer L, Switzer R, Watkins D (1976) Simultaneous demonstration of horseradish peroxydase and acetylcholinesterase. Neurosci Lett 3:1-15

Harting JK, Updyke BV, Van Lieshout DP (1992) Corticotectal projections in the cat: anterograde transport studies of twenty-five cortical areas. J Comp Neurol 324:379-414

Harting JK, Updyke BV, Van Lieshout DP (2001a) Striatal projections from the cat visual thalamus. Eur J Neurosci 14:893-896

Harting JK, Updyke BV, Van Lieshout DP (2001b) The visual-oculomotor striatum of the cat: functional relationship to the superior colliculus. Exp Brain Res 136:138-142

Henry G, Dreher B, Bishop PO (1974) Orientation specificity of cells in cat striate cortex. J Neurophysiol 37:1394-1409

Hicks TP, Benedek G, Thurlow GA (1988a) Modality specificity of neuronal responses within the cat's insula. J Neurophysiol 60:422-437

Hicks TP, Benedek G, Thurlow GA (1988b) Organization and properties of neurons in a visual area within the insular cortex of the cat. J Neurophysiol 60:397-421

Hikosaka O, Sakamoto M, Usui S (1989) Functional properties of monkey caudate neurons. II. Visual and auditory responses. J Neurophysiol 61:799-813

Hoshino K, Katoh YY, Bai W, Kaiya T, Norita M (2000) Distribution of terminals from pedunculopontine tegmental nucleus and synaptic organization in lateralis medialis-suprageniculate nucleus of cat's thalamus: anterograde tracing, immunohistochemical studies, and quantitative analysis. Vis Neurosci 17:893-904

Ikeda H, Wright MJ (1975) Spatial and temporal properties of "sustained" and "transient" neurones in area 17 of the cat's visual cortex. J Physiol 22:363-383

Jiang H, Lepore F, Ptito M, Guillemot JP (1994) Sensory modality distribution in the anterior ectosylvian cortex (AEC) of cats. Exp Brain Res 97:404-414

Katoh YY, Arai R, Benedek G (2000) Bifurcating projections from the cerebellar fastigial neurons to the thalamic suprageniculate nucleus and to the superior colliculus. Brain Res 864:308-311

Katoh YY, Benedek G, Deura S (1995) Bilateral projections from the superior colliculus to the suprageniculate nucleus in the cat: a WGA-HRP/double fluorescent tracing study. Brain Res 669:298-302

Katoh YY, Benedek G (1995) Organization of the colliculo-suprageniculate pathway in the cat: a wheat germ agglutinin-horseradish peroxidase study. J Comp Neurol 352:381-397

Katoh YY, Benedek G (2003) Cerebellar fastigial neurons send bifurcating axons to both the left and right superior colliculus in cats. Brain Res 970:246-249

Kolomiets B (1993) A possible visual pathway to the cat caudate nucleus involving the pulvinar. Exp Brain Res 97:317-324

Loe PR, Benevento LA (1969) Auditory-visual interaction in single units in the orbito-insular cortex of the cat. Electroencephalogr Clin Neurophysiol 26:395-398

Lokwan SJ, Overton PG, Berry MS, Clark D (1999) Stimulation of the pedunculopontine tegmental nucleus in the rat produces burst firing in A9 dopaminergic neurons. Neuroscience 92:245-254

McHaffie JG, Thomson CM, Stein BE (2001) Corticotectal and corticostriatal projections from the frontal eye fields of the cat: an anatomical examination using WGA-HRP. Somatosens Mot Res 18:117-130

Meredith MA, Stein BE (1986) Visual, auditory and somatosensory convergence on cells in superior colliculus results in multisensory integration. J Neurophysiol 56:640-662

Meredith MA, Wallace MT, Stein BE (1992) Visual, auditory and somatosensory convergence in output neurons of the cat superior colliculus: multisensory properties of the tecto-reticulo-spinal projection. Exp Brain Res 88:181-186

Miceli D, Reperant J, Ptito M (1985) Intracortical connections of the anterior ectosylvian and lateral suprasylvian visual areas in the cat. Brain Res 347:291-298

Middlebrooks JC, Clock AE, Xu L, Green DM (1994) A panoramic code for sound location by cortical neurons. Science 264:842-844

Middlebrooks JC, Xu L, Eddins AC, Green DM (1998) Codes for sound-source location in nontonotopic auditory cortex. J Neurophysiol 80:863-882

Middlebrooks JC, Xu L, Furukawa S, Macpherson EA (2002) Cortical neurones that localize sounds. Neuroscientist 8:73-83

Morrone MC, Di Stefano M, Burr DC (1986) Spatial and temporal properties of neurons of the lateral suprasylvian cortex of the cat. J Neurophysiol 56:969-986

Movshon JA, Thompson ID, Tolhurst DJ (1978) Spatial and temporal contrast sensitivity of neurones in areas 17 and 18 of the cat's visual cortex. J Physiol 283:101-120

Mucke L, Norita M, Benedek G, Creutzfeldt O (1982) Physiologic and anatomic investigation of a visual cortical area situated in the ventral bank of the anterior ectosylvian sulcus of the cat. Exp Brain Res 46:1-11

Niida T, Stein BE, McHaffie JG (1997) Response properties of corticotectal and corticostriatal neurons in the posterior lateral suprasylvian cortex of the cat. J Neurosci 17: 8550-8565

Norita M, Hicks TP, Benedek G, Katoh YY (1991) Organization of cortical and subcortical projections to the feline insular visual area, IVA. J Hirnforsch 32:119-134

Norita M, Mucke L, Benedek G, Albowitz B, Katoh YY, Creutzfeldt OD (1986) Connections of the anterior ectosylvian visual area (AEV). Exp Brain Res 62:225-240

Olson CR, Graybiel AM (1983) An outlying visual area in the cerebral cortex of the cat. Prog Brain Res 58:239-245

Olson CR, Graybiel AM (1987) Ectosylvian visual area of the cat: location, retinotopic organization, and connections. J Comp Neurol 261:277-294

Pinter RB, Harris LR (1981) Temporal and spatial response characteristics of the cat superior colliculus. Brain Res 207:73-94

Pouderoux C, Freton E (1979) Patterns of unit responses to visual stimuli in the cat caudate nucleus under chloralose anesthesia. Neurosci Lett 11:53-58

Redgrave P, Mitchell IJ, Dean P (1987) Descending projections from the superior colliculus in rat: a study using orthograde transport of wheatgerm-agglutinin conjugated horseradish peroxidase. Exp Brain Res 68:147-167

Reinoso-Suarez F, Roda JM (1985) Topographical organization of the cortical afferent connections to the cortex of the anterior ectosylvian sulcus in the cat. Exp Brain Res 59:313-324

Rolls ET, Thorpe SJ, Maddison SP (1983) Responses of striatal neurons in the behaving monkey. 1. Head of the caudate nucleus. Behav Brain Res 7:179-210

Rose D, Blakemore C (1974) An analysis of orientation selctivity in the cat's visual cortex. Exp Brain Res 20:1-17

Rosenquist AC (1985) Cerebral Cortex Volume 3 Visual Cortex. In: Peters A, Jones EG (eds.) Connenctions of visual Cortical Areas in the Cat. New York Plenum Press, New York, pp 81-117

Saul AB, Humphrey AL (1992) Temporal-frequency tuning of direction selectivity in cat visual cortex. Vis Neurosci 8:365-372

Scannell JW, Sengpiel F, Tovee MJ, Benson PJ, Blakemore C, Young MP (1996) Visual motion processing in the anterior ectosylvian sulcus of the cat. J Neurophysiol 76:895-907

Sherk H, Mulligan KA (1992) Retinotopic order is surprisingly good within cell columns in the cat's lateral suprasylvian cortex. Exp Brain Res 91:46-60

Snider RS, Niemer WT (1964) A stereotaxic atlas of the cat brain. University of Chicago Press, Chicago

Spear PD (1991) Functions of extrastriate visual cortex in non-primate species. In: Leventhal AG (ed) The neural basis of visual function. The Macmillan Press Ltd, London, pp 342-362

Stein BA, Meredith MA (1991) Functional organisation of the superior colliculus. In: Leventhal AG (ed) The neural basis of Visual Function. The Macmillan Press Ltd, London, pp 85-110

Stein BE, Meredith MA (1993) The Merging of the Senses. Cambridge MA. MIT Press, Cambridge

Stein BE, Wallace MT (1996) Comparisons of cross-modality integration in midbrain and cortex. Prog Brain Res 112:289-299

Sterling P, Wickelgren BG (1969) Visual receptive fields in the superior colliculus of the cat. J Neurophys 32:1-15

Strecker ER, Steinfels G, Abercrombie ED, Jacobs BL (1985) Caudate unit activity in freely moving cats: effects of phasic auditory and visual stimuli. Brain Res 329:350-353

Tamai Y, Miyashita E, Nakai M (1989) Eye movements following cortical stimulation in the ventral bank of the anterior ectosylvian sulcus of the cat. Neurosci Res 7:159-163

Tanaka K, Ohzawa I, Ramoa AS, Freeman RD (1987) Receptive field properties of cells in area 19 of the cat. Exp Brain Res 65:549-558

Tardif E, Bergeron A, Lepore F, Guillemot JP (1996) Spatial and temporal frequency tuning and contrast sensitivity of single neurons in area 21a of the cat. Brain Res 716:219-223

Tardif E, Lepore F, Guillemot JP (2000) Spatial properties and direction selectivity of single neurons in area 21b of the cat. Neuroscience 97:625-634

Tardif E, Richer L, Bergeron A, Lepore F, Guillemot JP (1997) Spatial resolution and contrast sensitivity of single neurons in area 19 of split-chiasm cats: a comparison with primary visual cortex. Eur J Neurosci 9:1929-1939

Tokuno H, Takada M, Ikai Y, Mizuno N (1994) Direct projections from the deep layers of the superior colliculus to the subthalamic nucleus in the rat. Brain Res 639:156-160

Tusa RJ, Palmer LA, Rosenquist AC (1978) The retinotopic organization of area 17 (striate cortex) in the cat. J Comp Neurol 177:213-235

von Grünau M, Frost BJ (1983) Double-opponent-process mechanism underlying RF-structure of directionally specific cells of cat lateral suprasylvian visual area. Exp Brain Res 49:84-92

Waleszczyk WJ, Wang C, Burke W, Dreher B (1999) Velocity response profiles of collicular neurons: parallel and convergent visual information channels. Neuroscience 93:1063-1076

Wallace MT, Meredith MA, Stein BE (1992) Integration of multiple sensory modalities in cat cortex. Exp Brain Res 91:484-488

Wallace MT, Stein BE (1996) Sensory organisation of the superior colliculus in cat and monkey. Prog Brain Res 12:301-311

Wang C, Dreher B, Assaad N, Ptito M, Burke W (1998) Excitatory convergence of Y and non-Y channels onto single neurons in the anterior ectosylvian visual area of the cat. Eur J Neurosci 10:2945-2956

Wang C, Waleszczyk WJ, Benedek G, Burke W, Dreher B (2001) Convergence of Y and non-Y channels onto single neurons in the superior colliculi of the cat. Neuroreport 12:2927-2933

Wilkinson LK, Meredith MA, Stein BE (1996) The role of anterior ectosylvian cortex in cross-modality orientation and approach behavior. Exp Brain Res 112:1-10

Wimborne BM, Henry GH (1992) Response characteristics of the cells of cortical area 21a of the cat with special reference to orientation specificity. J Physiol 449:457-478

Zumbroich TJ, Blakemore C (1987) Spatial and temporal selectivity in the suprasylvian visual cortex of the cat. J Neurosci 7:482-500

10. Figures and figure captions

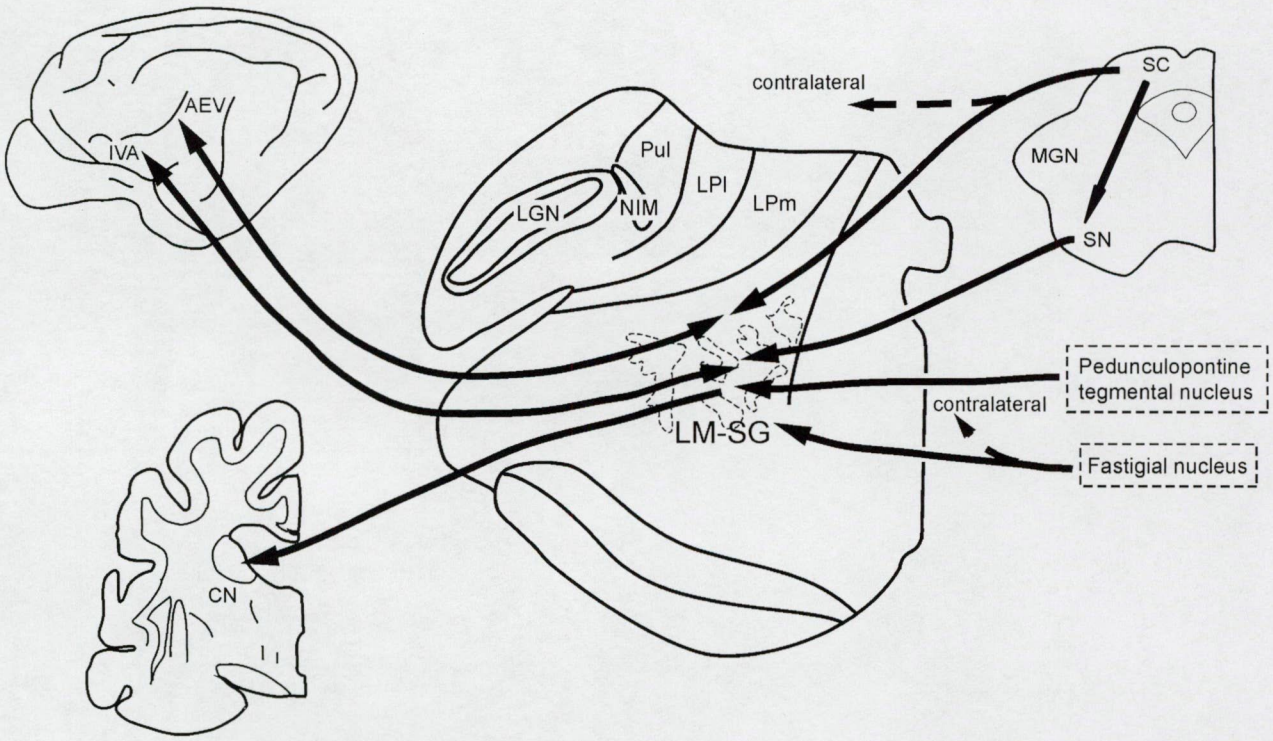

Figure 1.

Connections of extrastriatal visual cortical and subcortical structures in the feline brain. Abbreviations: AEV:anterior ectosylvian visual area, CN: caudate nucleus, IVA: insular visual area, LGN: lateral geniculate nucleus, LM-SG: lateralis medialis-suprageniculate nucleus, LPm: medial division of lateral posterior nucleus, LPl: lateral division of lateral posterior nucleus, Pul: pulvinar, SC: superior colliculus, SN: substantia nigra.

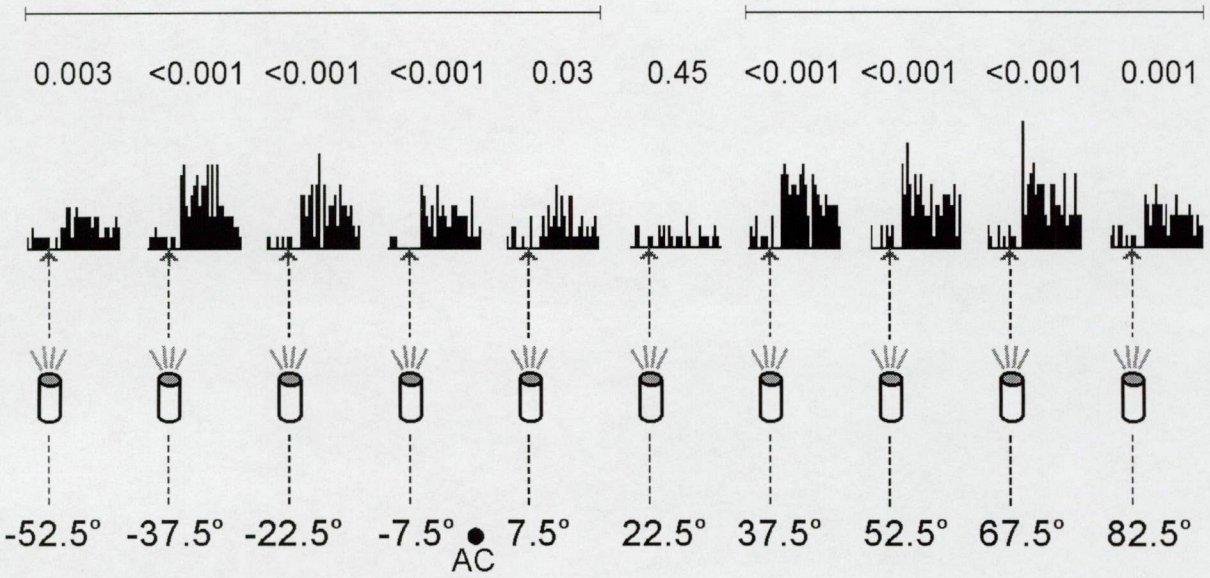

Figure 2.

Schematic drawing of the visual stimulating set-up (bottom) and PSTHs (middle) of a typical visual neuron along the AES. Schematic bulbs represent the positions of the LED diodes. Broken lines indicate the corresponding histograms and stimulus sites. The numbers in degrees denote the site of the visual stimulus related to the area centralis in the horizontal plane. The arrows below the PSTHs demonstrate the beginning of the visual stimulation (peristimulus time). The numbers above the PSTHs show the corresponding significance level of the t-test in which the prestimulus and peristimulus firing rates are compared. The lines at the top indicate the objectively estimated extent of the visual receptive field of this single neuron. Abbreviation: AC = area centralis

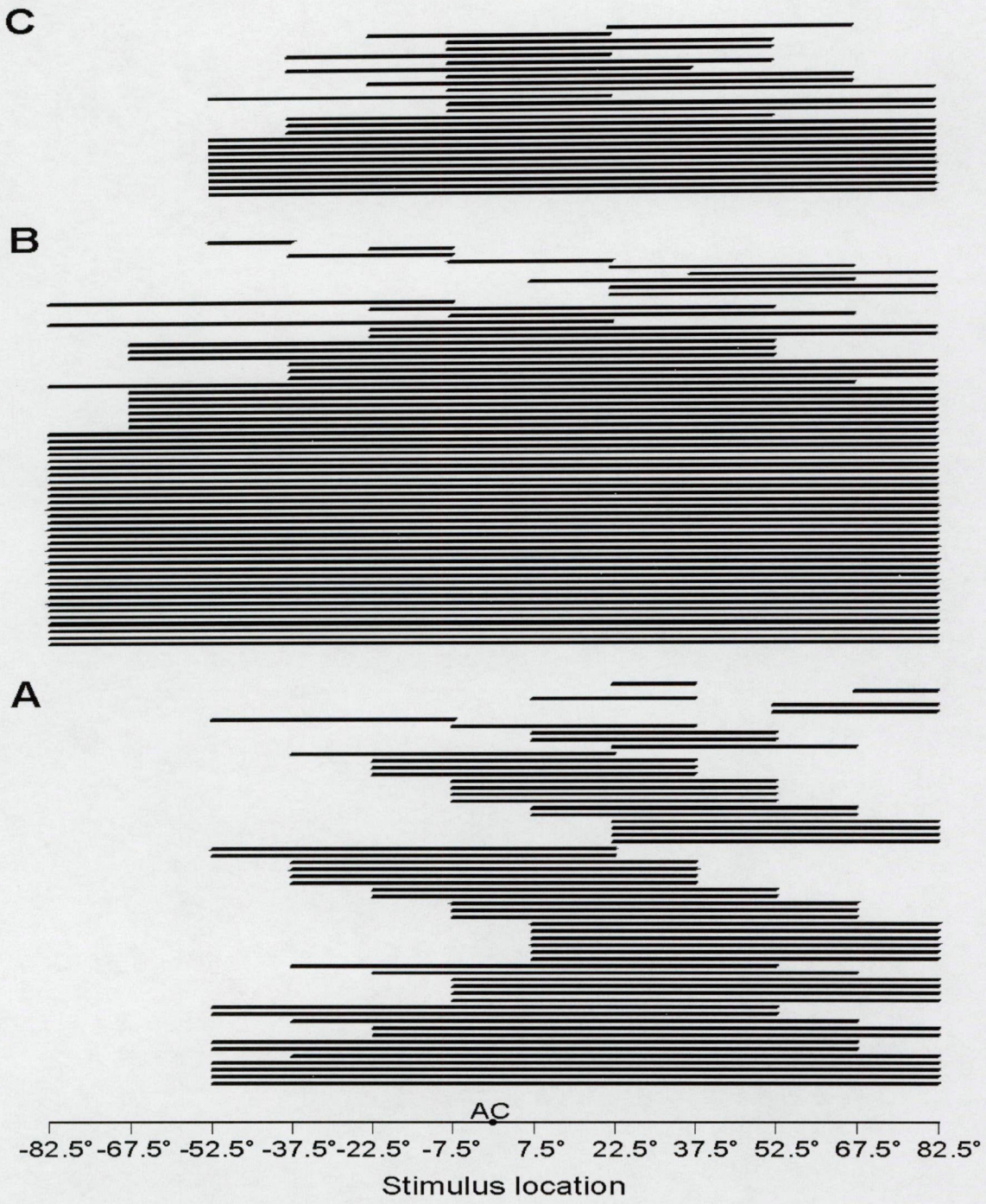

Figure 3.

The extents of 59 visual (A), 60 auditory (B) and 31 bimodal (both auditory and visual) receptive fields (C) of AES neurons estimated by our objective, statistical method. The numbers in degrees indicate the sites of the stimuli related to the area centralis in the horizontal plane. Horizontal lines reveal statistically significant increases in the firing rate as responses to stimulation in the corresponding part of the receptive field. Abbreviation: AC = area centralis

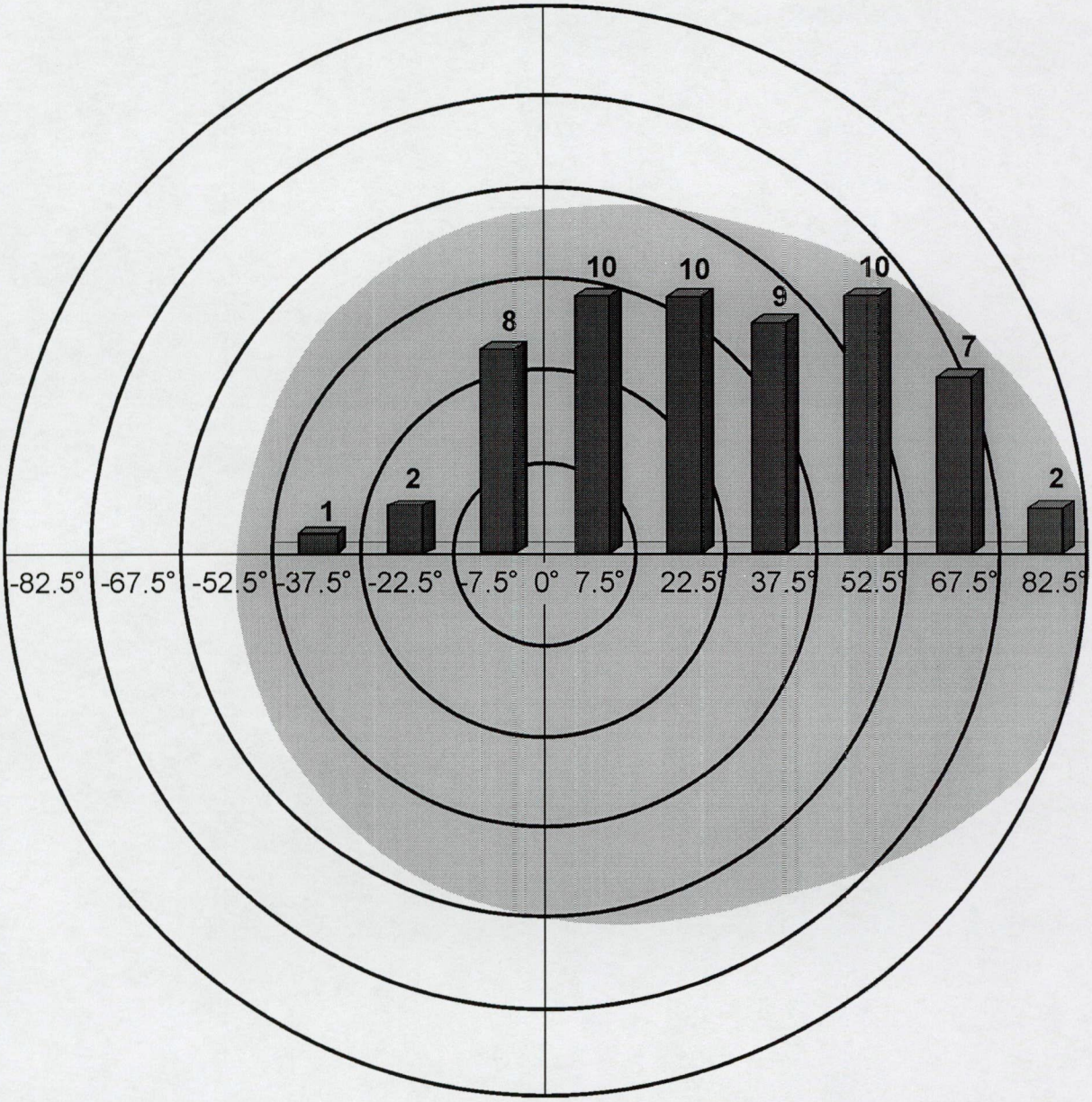

Figure 4.

The positions of sites maximally sensitive to visual stimulation in 59 AES neurons. The heights of the columns are proportional to the numbers of neurons (shown also in figures above) that displayed maximal sensitivities to stimuli at the corresponding part of the visual receptive field. The shaded area represents the visual field of the right eye.

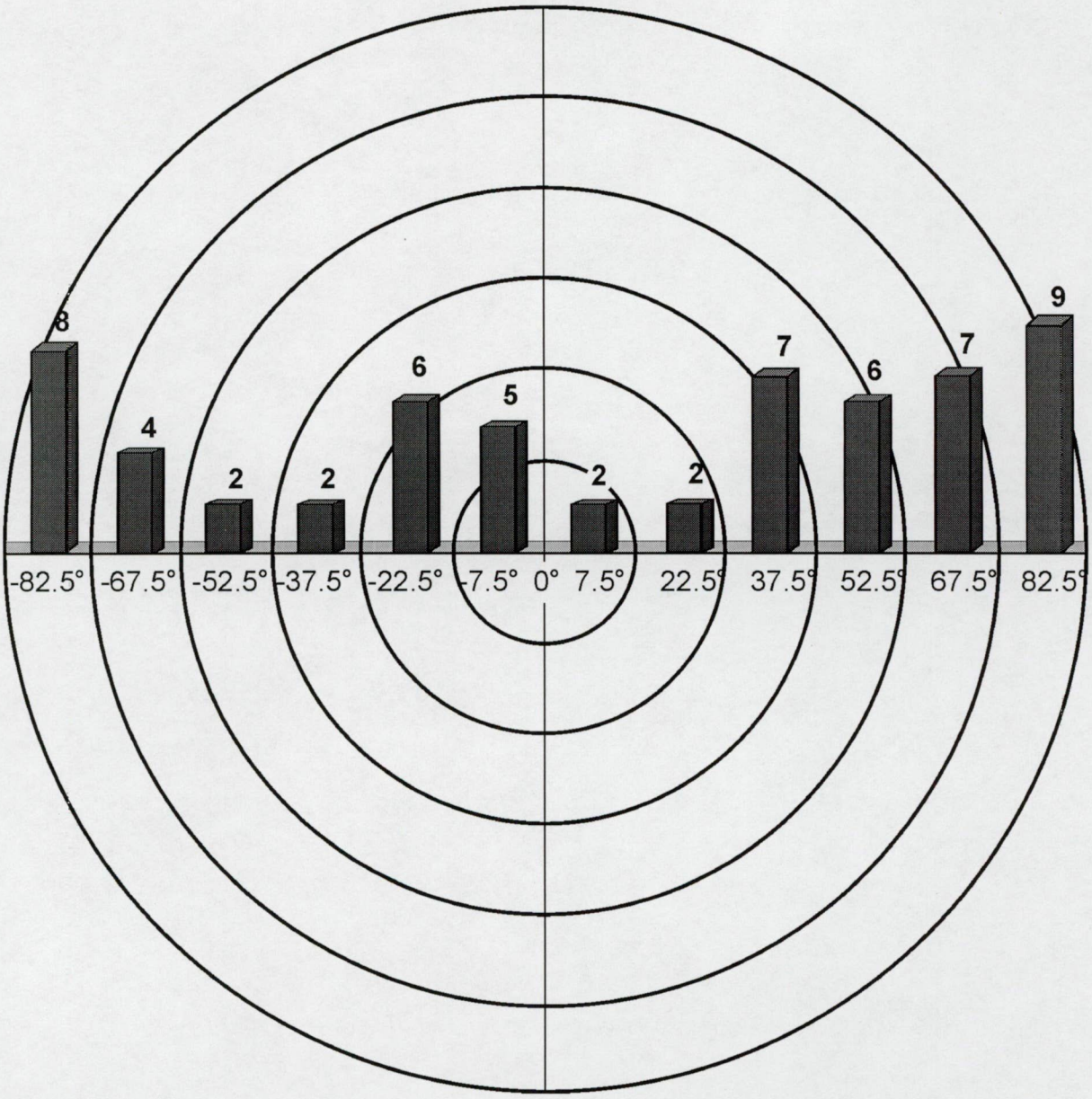

Figure 5.

The positions of sites maximally sensitive to auditory stimulation in 60 AES neurons. The heights of the columns are proportional to the numbers of neurons (shown also in figures above) that displayed maximal sensitivities to stimuli at the corresponding part of their auditory receptive field.

Figure 6.

The positions of sites maximally sensitive to visual-auditory (bimodal) stimulation of 31 AES neurons. The heights of the columns are proportional to the numbers of neurons (shown also in figures above) that displayed maximal sensitivities to stimuli at the corresponding part of their multimodal receptive field. The shaded area represents the visual field of the right eye.

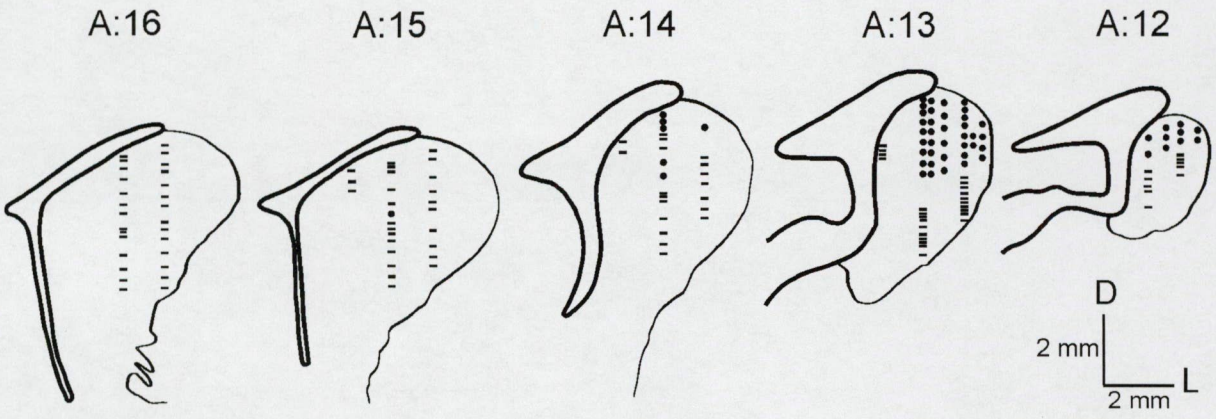

Figure 7.

Positions of visually responsive neurons (filled circles) and visually non-responsive neurons (minus signs) in the caudate nucleus. The drawings depict coronal sections of the caudate nucleus in the cat brain between A12 and A16 according to the stereotaxic atlas of Snider & Niemer (1964). Bars in the right bottom corner provide size calibration and orientation in the dorso-ventral and medio-lateral aspect.

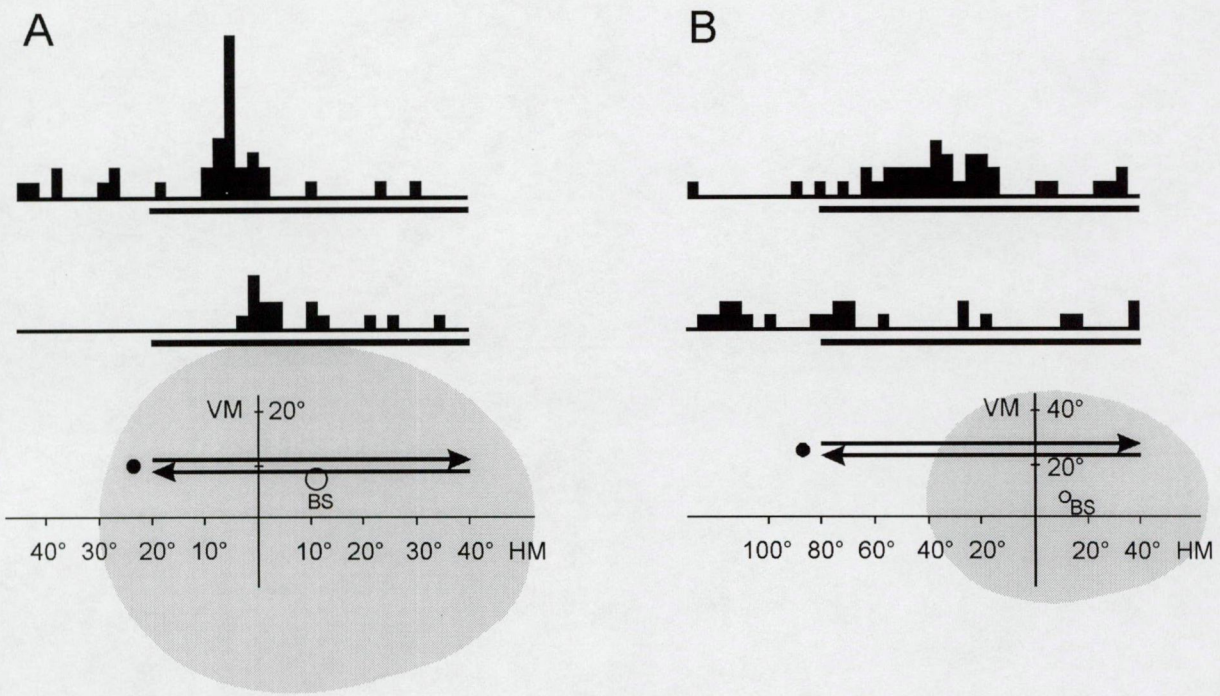

Figure 8.

Top: PSTHs demonstrating typical responses of the caudate neurons to moving visual stimuli. A: Responses of a directionally non-sensitive visual single unit. B: PSTHs of a direction-selective caudate single unit. The thick lines under the PSTHs indicate the duration of the stimulus movement (peristimulus time). Bottom: The position and movement of the stimulus in the visual field of the cat. Co-ordinates are given in degrees. The black spot left of the arrows symbolizes the start position of the moving visual stimulus. The upper and lower PSTHs correspond to the response of the neurons to the stimulus moving along the trace indicated by the upper and lower arrows, respectively. The shaded areas represent the visual receptive field of the caudate nucleus neurons estimated subjectively. Abbreviations: VM: vertical meridian, HM: horizontal meridian, BS: blind spot.

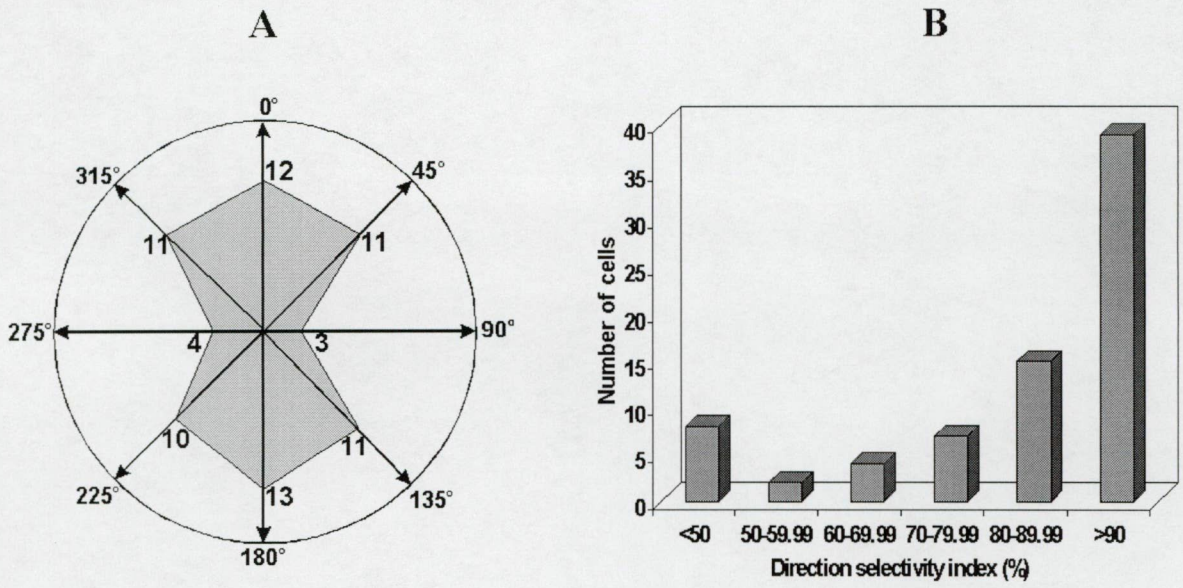

Figure 9.

The number of single neurons that showed preference for directions indicated by arrow (A). The stimuli were high-contrast (50%) sinewave gratings with constant spatial and temporal frequencies (0.2 c/deg and 6 Hz) drifting in 8 different directions from 0^{o} to 315^{o} at increments of 45^{o}. Note that most cells exhibited high direction selectivity indices (DI) of over 70% (B).

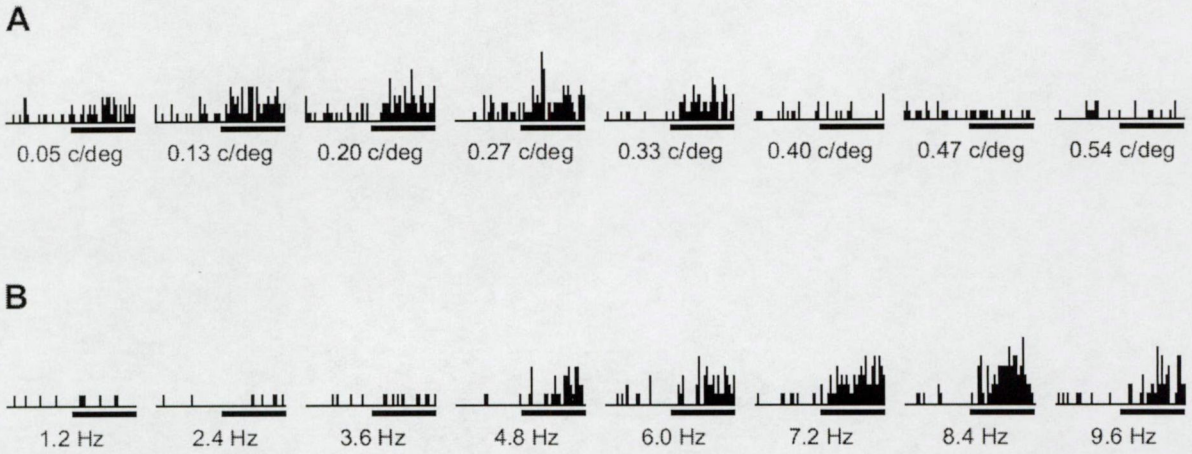

Figure 10.

PSTHs of a typical, band-pass tuned AEV single neurone to drifting sinusoidal modulated gratings with eight different spatial and temporal frequencies. A: Responses of an AEV unit to eight different spatial frequencies. The gratings were moved in the optimal direction of this unit. This neuron was responsive to spatial frequencies lower than 0.33 c/deg. The optimal spatial frequency of this unit was 0.27 c/deg. Under the PSTHs the corresponding spatial frequencies of the sinusoidally modulated gratings are displayed. The thick lines under the PSTHs indicate the duration of the stimulus movement (peristimulus time). B: Responses an AEV single neurone to eight different temporal frequencies. The gratings were moved in the optimal direction with an optimal spatial frequency of this neuron (0.27 c/deg). This unit elicited vigorous responses to temporal frequencies higher than 4.8 Hz. The optimal temporal frequency of this unit was 8.4 Hz. Under the PSTHs can be seen the corresponding temporal frequencies of the sinusoidally modulated gratings. The thick lines under the PSTHs indicate the duration of the stimulus movement.

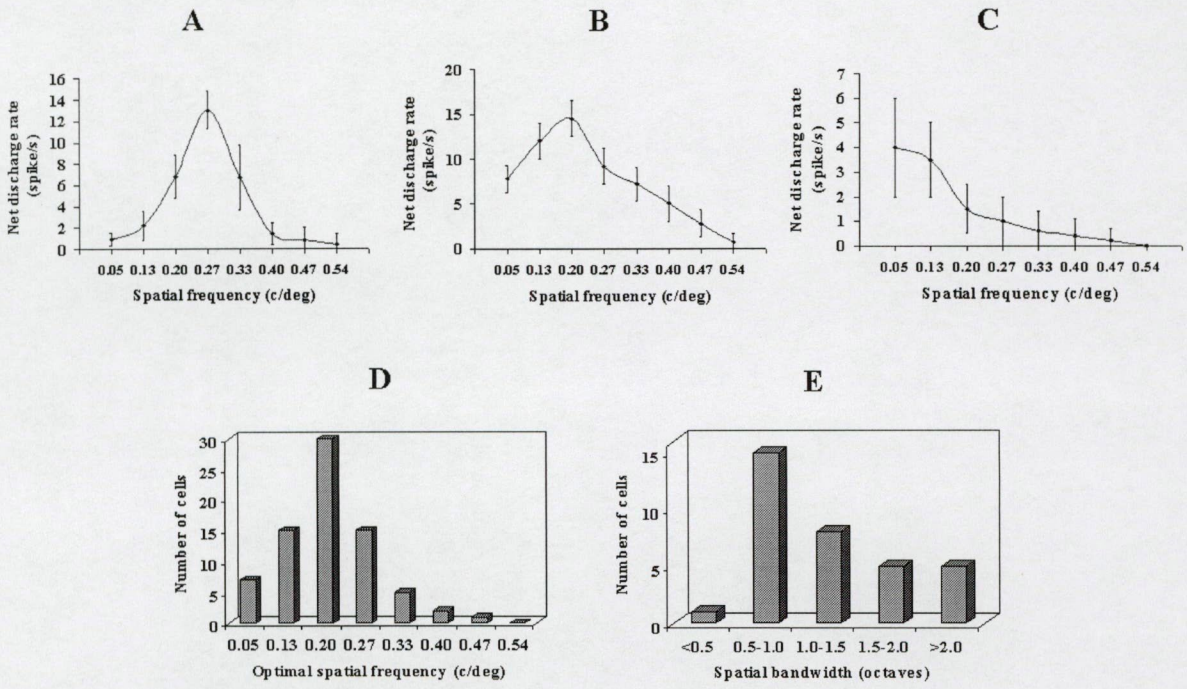

Figure 11.

Examples of typical spatial frequency tuning function. The stimulus was a high-contrast (50%) sinusoidal modulated grating drifting in the optimal direction of each unit. Each point corresponds to the mean net firing rate for a particular spatial frequency, which was varied in 8 steps from 0.05 c/deg to 0.54 c/deg. Vertical bars indicate SD values. The cells in A and B show band-pass tuning characteristics, while the cell in C is low-pass tuned to different spatial frequencies. D: Distribution of optimal spatial frequency estimated from the spatial frequency tuning functions. All cells responded optimally to relative low spatial frequencies. None of them had their maximal net discharge rate to spatial frequencies above 0.47 c/deg. E: Distribution of spatial bandwidths (full width at half-height). Most of the units are finely tuned to spatial frequencies, though a few of them display broader spatial tuning.

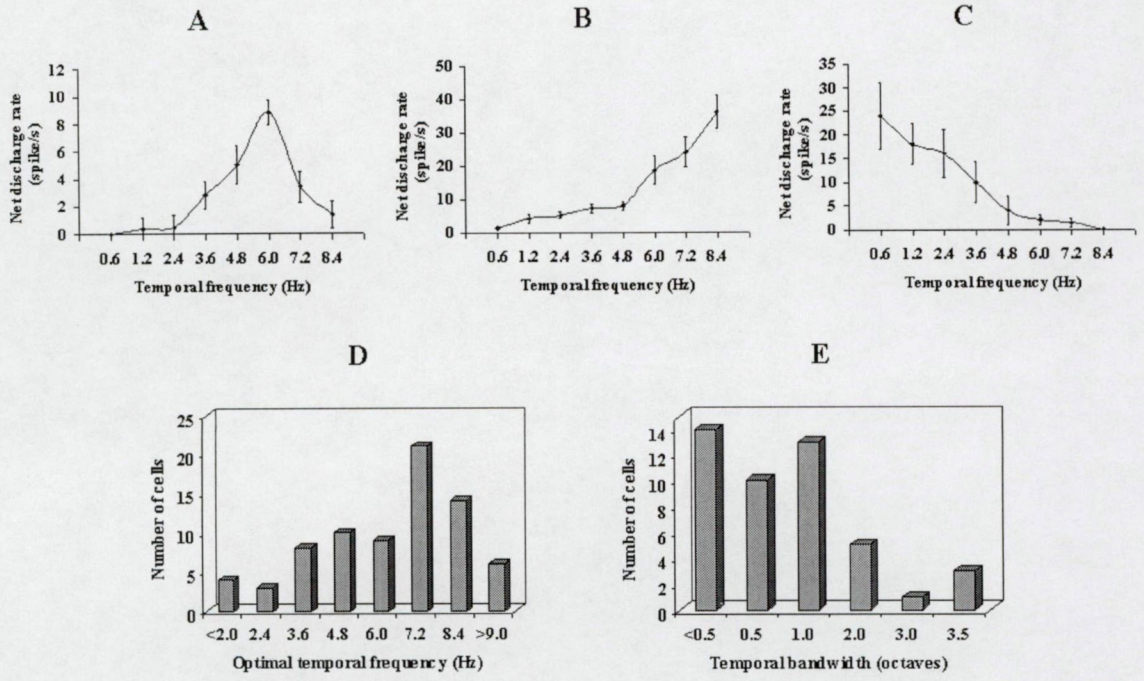

Figure 12.

Examples of typical temporal frequency tuning function. The stimulus was a high-contrast (50%) sinewave grating of optimal spatial frequency drifting in the optimal direction of each unit. Each point corresponds to the mean net firing rate for a particular temporal frequency. Vertical bars show the SD values. The cell in A showed a temporal band-pass function that in B exhibited a temporal high-pass function, while the unit in C exhibited a temporal low-pass function. D: Distribution of optimal temporal frequencies of cells, estimated from the temporal frequency tuning functions. Most of the cells responded optimally to high temporal frequencies though cells were also found that showed preferences for all examined temporal frequencies between 0.6 Hz and 10.8 Hz. E: Distribution of temporal bandwidths (full width at half-height). Most of the cells exhibited very fine temporal tuning, but a few of them were broadly tuned to temporal frequencies.